was 5.35 Å. This turn had a nearly type I β-turn conformation from the viewpoint of the dihedral angles of constructing residues. However, no NMR information about the hydrogen bonding was obtained, and furthermore it was clarified that there was no intra-turn hydrogen bond in the calculated structures. This turn was therefore defined as a $\beta_{E}\gamma$-type turn,[14] that is, a type-IV β-turn (miscellaneous type) according to the classical nomenclature. The second turn was a helical turn like the conformation of the 3_{10} helix. The C-terminal region of p3 showed a highly disordered structure absent from GM1, therefore this region might play an important role in binding to GM1 saccharides.

2.3. Molecular dynamics study for the p3

Molecular dynamics (MD) simulations were also carried out. Two major structures were obtained with the MD calculations within 40 ns at 325 K, preceded by the MD to generate the starting geometries at high temperature. These were in good agreement with the fluctuating conformations obtained by NMR experiments. One of these had a curb form at the middle of p^3, Pro^7–Phe^9, and there were no characteristic hydrogen bonds in half of the N-terminus, which meant that the peptide did not have a specific secondary structure (Fig. 7). Although the RMSD between the structures from the NMR study and the MD simulation was large (4.67 Å), both structures had the same topology. This suggested that the MD simulations were able to support

Figure 7. Superimposed structure of p3 from MD simulations (green) and from NMR data without GM1. Both have the same topologies including (i) curb structure at the middle and (ii) no secondary structure although MD simulation showed 'helix-like' predicted structure at the C-terminal area. Side chains of key residues that bind GM1, Pro^7–Phe^9 and Trp^2, are also shown.

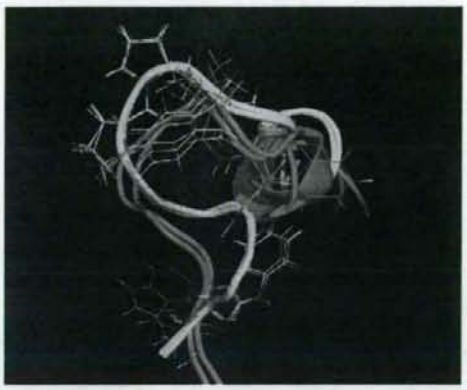

Figure 8. Superimposed structure of p3 from MD simulations (green) and from NMR data with GM1. Although the MD calculations were performed without any ligand, the structure from MD was similar to the structure from NMR with GM1. Side chains of key residues that bind GM1, Pro^7–Phe^9 and Trp^2, are also shown.

the NMR experiments. Figure 8 shows the other structure obtained by MD with the bound p3 NMR backbone structure. Although we have not considered the existence of GM1 during these simulations, we found that the RMSD for the backbone structure of 3.56 Å was smaller than the case in Figure 8.

3. Discussion

In summary, the structure of the p3 peptide was stabilized completely in the presence of the GM1 oligosaccharide, which existed in the micelle form. In the bound form, the peptide is stabilized by forming stable β- and helical turns, whereas the Pro^7–Pro^8 region contributing to the bend in the peptide structure was preserved.[15,16] Therefore, it can be suggested that the N- and the C-terminal regions underwent drastic conformational change upon the binding of the GM1 pentasaccharide (Fig. 6). Unfortunately, no characteristic intermolecular NOEs that could suggest a specific binding site were observed in this study because GM1 formed micelles in aqueous solution and thus gave significant line-broadening in the NMR spectra.

Previous studies on lectins proposed that the modular structure of the aromatic ring of tryptophan on the β-turn, known as the carbohydrate-binding module (CBM), plays a key role in the hydrophobic interaction with the nonpolar face of monosaccharide rings.[17–19] Based on the structural analyses of p3, Trp^2 of the bound state was also included in the β-turn and constructed a hydrophobic core. We, therefore, propose that Trp^2 would be an essential residue for binding to

GM1 pentasaccharide. Moreover, for the representative example of the recognition of NeuAc, arginine binds to the carboxyl group of NeuAc through the electrostatic interaction in the coat protein of murine polyoma virus.[20] This GM1-binding peptide had two arginines, Arg^3 and Arg^{12}, located on the β-turn and the helical turn, respectively. From the viewpoint of the solution structure of the bound state, the side chain of Arg^{12} was exposed to solvent with more disordered direction than that of Arg^3, which would suggest that Arg^3 is strongly involved in the recognition of NeuAc in GM1.

Although Honda et al. reported the conformation of a 10 amino acid residual peptide,[21] it is difficult, in general, for a small peptide to form a steady conformation and create a stable binding site for oligosaccharides in aqueous solution. Thus our results indicate that the structure of ligand peptide was controlled by the carbohydrate platform. Whereas it is frequently reported that gangliosides on the cell surface behave as receptors to various ligands, we believe that the regulation of the protein and peptide structure is also one of the most essential functions of carbohydrates. As another interesting study on ganglioside–peptide interaction, it has also been reported that enkephalins, endogenous neurotransmitters consisting of five amino acids have altered folding in the bound state with GM1 micelle.[22] This study indicated that enkephalins had an induced rigid turn structure by interaction with the GM1 micelle, which was very similar with the structure in bicelles.[23] Moreover, the nonapeptide bradykinin, a neuropeptide with an antiphlogistic effect, was also recently confirmed to undergo conformational change on binding to GM1 micelles.[24] These drastic transitions of the structure of ligand peptide on GM1 surface are likely to play an important role in the ignition of sequential events like the traditional pathway of cholera toxin infection.

4. Experimental

4.1. General

Unless otherwise stated, all commercially available solvents and reagents were used without further purification. Fmoc amino acid derivatives and resin were purchased from NOVA Biochem Co. Ltd. Automatic peptide synthesis was performed with Advanced Chem Tech MODEL Apex396 peptide synthesizer. HPLC was performed on a Hitachi HPLC system equipped with an L-7150 intelligent pump, an L-7420 UV detector and reversed-phase C18 column, Inertsil® ODS-3 (20 × 250 mm) at a flow rate of 5.0 mL min^{-1}. The eluate was monitored by UV absorption at 220 nm. MALDI-TOF MS analyses were performed with the Bruker REFLEXIII mass spectrometry with 2,5-dihydroxybenzoic acid (DHB).

4.2. Preparation of samples

GM1 was purchased from Wako Pure Chemical Industries, Ltd. (Osaka, Japan) and was used without further purification.

The p3 peptide, VWRLLAPPFSNRLLP,[9,10] was synthesized on Fmoc-Pro-OH preloaded 2-chlorotrityl chloride resin (0.66 mmol/g) using an automatic peptide synthesizer (a common solid-phase peptide synthetic method with Fmoc strategy) in four batches on 0.02 mmol scale each (four portions of 30 mg of preloaded resin each). Fmoc amino acid derivatives, Fmoc-Pro-OH, Fmoc-Leu-OH, Fmoc-Arg(Pbf)-OH, Fmoc-Asn(Trt)-OH, Fmoc-Ser(*t*Bu)-OH, Fmoc-Phe-OH, Fmoc-Ala-OH, Fmoc-Trp(Boc)-OH and Fmoc-Val-OH, were employed. A cycle of automated peptide synthesizer for a 0.02 mmol scale was defined as follows. The resin was treated with 1.5 mL of 20% (v/v) piperidine in DMF and the mixture was stirred for 5 min at ambient temperature. After filtration, the same process was performed but stirred for 15 min. Then, the resin was washed with NMP (*N*-methylpyrrolidine, 1.5 mL) and DMF (1.5 mL). To a mixture of a solution of Fmoc amino acid (4 equiv) and HOBt (*N*-hydroxybenzotriazole, 3.5 equiv) in NMP (600 μL) and a solution of HBTU (2-(1*H*-benzotriazole-1-yl)-1,1,3,3-tetramethyluronium hexafluorophosphate, 4 equiv) and DIEA (diisopropylethylamine, 6 equiv) in DMF (600 μL) was added the resin, and the reaction mixture was stirred for 40 min at ambient temperature. This coupling process was performed twice. After washing the resin with NMP (1.5 mL) and DMF (1.5 mL), nonreactive amino groups were acetyl-capped with 1.5 mL of a mixed solution of Ac_2O (4.75% as v/v) and HOBt (13 mM) in NMP. After completing the peptide synthesis process, the resin was washed with NMP (1.5 mL) and CH_2Cl_2 (1.5 mL), and dried in vacuo. The protected peptide on the resin was treated with 10 mL of a mixed solution of TFA/H_2O/ethanedithiol/triisopropylsilane (94.5/2.5/2.5/1.0 (v/v/v/v)) for 3 h at ambient temperature followed by washing with TFA (2 mL) to remove the peptide from resin and for deprotection of protecting groups such as -*t*Bu, -Trt, -Pbf, and -Boc. The combined solvent was dried with blowing N_2 gas and precipitated from cold dry *tert*-butylmethyl ether. The obtained white solid was purified by HPLC [eluate: solvent A (0.1% TFA in H_2O) and solvent B (0.1% TFA in acetonitrile), gradient; increase from 2% to 60% of B over 60 min]. The fractions containing the desired peptide were collected and lyophilized. The p3 peptide was obtained as a white powder (72 mg, 50% overall yield). Typical NMR data are shown in the figures. Amino acid analysis (theoretical ratio): Asp (Asn) 1.0 (1), Ser 0.8 (1), Ala 1.0 (1), Val 0.9 (1), Leu 4.0 (4), Phe 1.0 (1), Trp 0.9 (1), Arg 2.1 (2); MALDI-TOF-MS calcd for $[M+H]^+$ 1779.043, found $[M+H]^+$ 1779.827.

4.3. NMR measurements

Sample solutions for NMR measurements were prepared by dissolving p3 in a mixed solvent of 10% D_2O, 90% H_2O or 99.9% D_2O, and the sample pH was adjusted to 4.1. All NMR spectra were measured on a Bruker Avance 600 spectrometer equipped with a cryoprobe system operating at 600.13 MHz for the proton frequency. The sample was not spun and the spectra were recorded at a temperature of 300 K. Data acquisition was performed with XWINNMR 3.1 (Bruker) software operating on a Silicon Graphics O2+ workstation. The water signal was suppressed by low-power irradiation during the relaxation delay time and WATERGATE method with 3–9–19 pulse sequence with x, y, z-triple gradient.[25,26] One-dimensional ^{1}H NMR experiments were performed with a spectral width of 6009.615 Hz, 32K data points and 8 scans. Two-dimensional DQF–COSY,[27] TOCSY,[28,29] ROESY,[30] and NOESY[31] measurements were recorded in a phase sensitive mode. The TOCSY transfer was achieved with the MLEV-17 pulse sequence with spin-locking times of 60, 80, and 100 ms. ROESY and NOESY spectra were recorded with mixing times of 150 and 250 ms, respectively. Except for DQF–COSY determination of the $^3J_{HN\alpha}$, all two-dimensional measurements were recorded with 2048 × 512 frequency data points and zero-filled to yield 2048 × 2048 data matrices. High-resolution DQF–COSY experiments were measured with 4096 × 512 points and zero-filled to a 8192 × 8192 matrix with a 0.73 Hz point resolution. The number of scans for all spectra was 8. The time domain data in both dimensions were multiplied by a sine bell window function with 90° phase shift prior to Fourier transformation. All NMR spectra were processed by software NMRPIPE,[32] and the signals were assigned with the XEASY[33] program on a Silicon Graphics O2 workstation.

4.4. Structure modeling based on NMR data

Three-dimensional structures of p3 were calculated with CNS 1.1[34] program on a Linux workstation. A total of 114 and 146 distance restraints for p3 and the complex of the p3 and GM1 samples, respectively, were used to calculate the family of structures. Moreover, 12 dihedral angle ϕ restraints were used for both sample calculations. Distance restraints for calculations were estimated from the cross-peak intensities in ROESY or NOESY spectra with a mixing time of 150 ms; the estimated restraints were then classified as strong, medium, weak, and very weak, and assigned upper limits of 2.7, 3.5, 5.0, and 6.0 Å, respectively. Pseudo-atom corrections were used for unresolved NOE cross-peaks, methyl protons as well as nonstereospecifically assigned methylene and aromatic protons. In addition, 0.5 Å was added to the upper limit of the distance constraints of only the involved methyl protons according to the report by Clore et al.[35] The restraints of the dihedral angle ϕ were based on $^3J_{HN\alpha}$ coupling constants measured in high-resolution DQF–COSY. For checking of the restraints violation, the PROCHEK-NMR 3.5.4[36] program was used on a Linux workstation, and superimposition of the obtained structures, calculation of RMSD values, and general analyses of GM1-binding peptide were performed with MOLMOL[37] software.

4.5. Ab initio computational structural analysis with molecular dynamics simulation

A molecular dynamics simulation was performed with the AMBER software package version 8.0, using the third-generation point-charge all-atom force field for proteins, also known as ff03.[38] The solvents were implicitly represented by a generalized Born solvent model[39] with no cutoff. p3 was constructed with an extended feature using SYBYL Version 6.9 (Tripos Association, St. Louis, MO).

To generate a variety of conformations of p3 as a starting geometry, 500 steps of a molecular dynamics calculation at 900 K with 2 fs time steps were performed. For all structures, the temperature was gradually lowered until the RMS of the Cartesian elements of the gradient was <0.4 kcal/mol Å. Six groups of conformations were obtained and applied in additional MD calculations. Using each conformer as the starting structures, the 40 ns MD with Berendsen's algorithm[40] was carried out. The temperature and the pressures were kept at 325 K and 1 atm, respectively. In this simulation, the integration time step was 2.0 fs, and SHAKE[41] was applied to constrain all bonds connecting hydrogen atoms. The trajectories were saved every 5.0 ps. A total of 48,000 snapshots were sampled and two major conformers were obtained by a cluster analysis,[42] which are shown in Figures 7 and 8. AMBER 8.0 and PROCHECK were used to analyze the trajectories, and simulations were performed on HP GS1280, Sun Fire 12K, IBM p690, and a Linux cluster with 12 Pentium IV (2 GHz) CPUs.

Acknowledgments

The authors thank Professor Jesús Jiménz-Barbero, Centro de Investigaciones Biologicas, Madrid, Spain, for providing the opportunity to participate in this special issue of Carbohydrate Research on Glycomimetics, and Dr. Nobuaki Nemoto, JEOL Ltd., Akishima, Japan, for useful discussion.

References

1. Gabius, H.-J.; Siebert, H.-C.; André, S.; Jiménez-Barbero, J.; Rüdiger, H. *ChemBioChem* **2004**, *5*, 740–764.

2. Tugarinov, V.; Muhandiram, R.; Ayed, A.; Kay, L. E. *J. Am. Chem. Soc.* **2002**, *124*, 10025–10035.
3. Fiaux, J.; Bertelsen, E. B.; Horwich, A. L.; Wüthrich, K. *Nature* **2002**, *418*, 207–211.
4. Vyas, A. A.; Schnaar, R. L. *Biochimie* **2001**, *83*, 677–682.
5. Lloyd, K. O.; Furukawa, K. *Glycoconjugate J.* **1998**, *15*, 627–636.
6. Suzuki, Y. *Prog. Lipid Res.* **1994**, *33*, 429–457.
7. Hakomori, S. *Annu. Rev. Biochem.* **1981**, *50*, 733–764.
8. Iwabuchi, K.; Yamamura, S.; Prenetti, A.; Handa, K.; Hakomori, S. *J. Biol. Chem.* **1998**, *273*, 9130–9138.
9. Matsubara, T.; Ishikawa, D.; Taki, T.; Okahata, Y.; Sato, T. *FEBS Lett.* **1999**, *456*, 253–256.
10. Matsubara, T.; Iijima, K.; Nakamura, M.; Taki, T.; Okahata, Y.; Sato, T. *Langmuir* **2007**, *23*, 708–714.
11. Wüthrich, K. *NMR of Proteins and Nucleic Acids*; John Wiley and Sons: New York, 1986.
12. Basu, A.; Glew, R. H. *J. Biol. Chem.* **1985**, *260*, 13067–13073.
13. Lewis, P. N.; Momany, F. A.; Scheraga, H. A. *Biochim. Biophys. Acta* **1973**, *303*, 211–229.
14. Wilmot, C. M.; Thornton, J. M. *Protein Eng.* **1990**, *3*, 479–493.
15. Espinosa, J. F.; Gellman, S. H. *Angew. Chem., Int. Ed.* **2000**, *39*, 2330–2333.
16. Aemissegger, A.; Kräutler, V.; van Gunsteren, W. F.; Hilvert, D. *J. Am. Chem. Soc.* **2005**, *127*, 2929–2936.
17. Tormo, J.; Lamed, R.; Chirino, A. J.; Morag, E.; Bayer, E. A.; Shoham, Y.; Steitz, T. A. *EMBO J.* **1996**, *15*, 5739–5751.
18. Din, N.; Forsythe, I. J.; Burntnick, L. D.; Gilkes, N. R.; Miller, R. C., Jr.; Warren, R. A.; Kilburn, D. G. *Mol. Microbiol.* **1994**, *11*, 747–755.
19. Nagy, T.; Simpson, P. J.; Williamson, M. P.; Hazlewood, G. P.; Gilbert, H. J.; Orosz, T. A. *FEBS Lett.* **1998**, *429*, 312–316.
20. Stehle, T.; Yan, Y.; Benjamin, T. L.; Harrison, S. C. *Nature* **1994**, *369*, 160–163.
21. Honda, S.; Yamasaki, K.; Sawada, Y.; Morii, H. *Structure* **2004**, *12*, 1507–1518.
22. Chatterjee, C.; Mukhopadhyay, C. *Biopolymers* **2003**, *70*, 512–521.
23. Marcotte, I.; Separovic, F.; Auger, M.; Gagné, S. M. *Biophys. J.* **2004**, *86*, 1587–1600.
24. Chatterjee, C.; Mukhopadhyay, C. *Biochem. Biophys. Res. Commun.* **2004**, *315*, 866–871.
25. Piotto, M.; Saudek, V.; Sklenář, V. *J. Biomol. NMR* **1992**, *2*, 661–666.
26. Sklenár, V.; Piotto, M.; Leppik, R.; Saudek, V. *J. Magn. Reson. A* **1993**, *102*, 241–245.
27. Rance, M.; Sørensen, O. W.; Bodenhausen, G.; Wagner, G.; Ernst, R. R.; Wüthrich, K. *Biochem. Biophys. Res. Commun.* **1983**, *117*, 479–485.
28. Braunschweiler, L.; Ernst, R. R. *J. Magn. Reson.* **1983**, *53*, 521–528.
29. Bax, A.; Davis, D. G. *J. Magn. Reson.* **1985**, *65*, 355–360.
30. Bothner-By, A. A.; Stephens, R. L.; Lee, J.-M.; Warren, C. D.; Jeanloz, R. W. *J. Am. Chem. Soc.* **1984**, *106*, 811–813.
31. Jeener, J.; Meier, B. N.; Bachmann, P.; Ernst, R. R. *J. Chem. Phys.* **1979**, *71*, 4546–4553.
32. Delaglio, F.; Grzesiek, S.; Vuister, G.; Zhu, G.; Pfeifer, J.; Bax, A. *J. Biomol. NMR* **1995**, *6*, 277–293.
33. Bartels, C.; Xia, T. H.; Billeter, M.; Güntert, P.; Wüthrich, K. *J. Biomol. NMR* **1995**, *6*, 1–10.
34. Brünger, A. T.; Adams, P. D.; Clore, G. M.; DeLano, W. L.; Gros, P.; Grosse-Kunstleve, R. W.; Jiang, J.-S.; Kuszewski, J.; Nilges, M.; Pannu, N.; Read, R. J.; Rice, L. M.; Simonson, T.; Warren, G. L. *Acta Crystallogr., Sect. D* **1998**, *54*, 905–921.
35. Clore, G. M.; Gronenborn, A. M.; Nilges, M.; Ryan, C. A. *Biochemistry* **1987**, *26*, 8012–8023.
36. Laskowski, R. A.; Rullmann, J. A. C.; MacArthur, M. W.; Kaptein, R.; Thornton, J. M. *J. Biomol. NMR* **1996**, *8*, 477–486.
37. Koradi, R.; Billeter, M.; Wüthrich, K. *J. Mol. Graph.* **1996**, *14*, 51–55.
38. Duan, Y.; Wu, C.; Chowdhury, S.; Lee, M. C.; Xiong, G.; Zhang, W.; Yang, R.; Cieplak, P.; Luo, R.; Lee, T.; Caldwell, J.; Wang, J.; Kollman, P. *J. Comput. Chem.* **2003**, *24*, 1999–2012.
39. Onufriev, A.; Bashford, D.; Case, D. A. *Proteins: Struct. Funct. Bioinf.* **2004**, *55*, 383–394.
40. Berendsen, H. J. C.; Postma, J. P. M.; van Gunsteren, W. F.; DiNola, A.; Haak, J. R. *J. Chem. Phys.* **1984**, *81*, 3684–3690.
41. Ryckaert, J.-P.; Ciccotti, G.; Berendsen, H. J. C. *J. Comput. Phys.* **1977**, *23*, 327–341.
42. Jang, S.; Kim, E.; Shin, S.; Pak, Y. *J. Am. Chem. Soc.* **2003**, *125*, 14841–14846.

In Vitro Gene Delivery by pDNA/Chitosan Complexes Coated with Anionic PEG Derivatives that Have a Sugar Side Chain

Mayu Hashimoto,[1] Yoshiyuki Koyama,[2] and Toshinori Sato*[1]
[1]*Faculty of Science and Technology, Keio University, 3-14-1 Hiyoshi, Kouhoku-ku, Yokohama 223-8522*
[2]*Department of Home Economics, Otsuma Women's University, Chiyoda-ku, Tokyo 102-8357*

(Received December 10, 2007; CL-071368; E-mail: sato@bio.keio.ac.jp)

We developed pDNA/chitosan complexes coated with sugar-modified PEG-A/Cs, which are poly(ethylene glycol) derivatives with a side chain of carboxylic acid and sugar. The cationic pDNA/chitosan complexes were coated with anionic sugar-modified PEG-Cs, and anionic ternary complexes were formed. Coating the pDNA/chitosan complexes with maltose- or lactose-modified PEG-A/C (Mal–PEG-A/C or Lac–PEG-A/C, respectively) greatly promoted their stability in water and transfection efficiency in vitro.

A number of cationic polymers have been developed to deliver exogenous genes into cells. Chitosan is a naturally occurring polysaccharide showing low cytotoxicity, biocompatibility, and biodegradability,[1] and is often employed as a gene carrier. Sato et al. reported that DNA/chitosan complexes were uptaken into tumor cells, but not into blood monocytes.[2] Plasmid DNA (pDNA)/chitosan also showed high-level transfection efficiency both in vitro[3] and in vivo.[4] However, the stability of pDNA/chitosan complexes in water was low by self-aggregation and BSA-induced aggregation. To improve the stability and cell-specificity of the pDNA complexes, lactose- and mannose-modified chitosans have been developed as gene carriers.[5]

Poly(ethylene glycol), PEG, has been widely employed for drug delivery systems to prevent non-specific interaction with serum protein and cells. Conjugation of PEG to pDNA/polyethyleneimine (PEI) complexes resulted in a prolonged circulation time after intravenous injection.[6] The conjugation of PEG to pDNA/chitosan complexes increased the stability in water.[7] However, such a conjugation of PEG to the pDNA/chitosan complexes did not enhance their transfection efficiency.

In this study, we employed PEG derivatives with carboxylic acid and sugar moieties (sugar–PEG-A/Cs) as side chains to coat DNA/chitosan complexes. Anionic sugar–PEG-A/Cs form ternary complexes electrostatically with cationic pDNA/chitosan complexes (Figure 1). Sugar–PEG-A/Cs have been employed to coat pDNA/PEI complexes and enhance transfection efficiency.[8] However, it has been reported that PEI induced strong cytotoxicity.[9] The toxicity of a pDNA/PEI complex was about seven times higher than that of a pDNA/chitosan complex.[10] Therefore, in this study, we prepared pDNA/chitosan/sugar–PEG-A/C ternary complexes and evaluated their transfection efficiency in vitro.

Chitosan was obtained from Yaizu Suisankagaku Industry (Shizuoka, Japan). The average molecular weight was 40000, and the degree of deacetylation was 85%. PEG-A/C and sugar–PEG-A/Cs were synthesized according to a previous paper.[8] The substitution degrees of maltose and lactose were 2.9 and 4.4 per molecule, respectively (Figure 1). The molecular weight of Mal–PEG-A/C was 9770, and that of Lac–PEG-A/C was

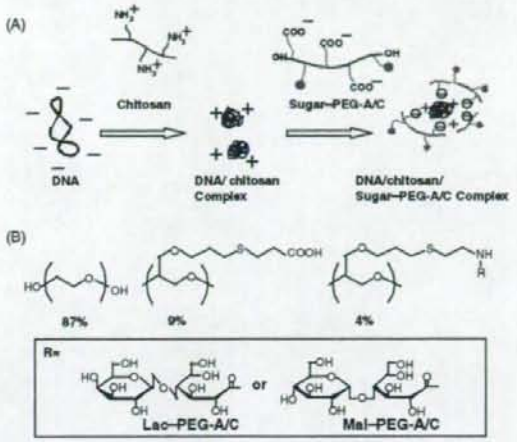

Figure 1. (A) A scheme for the formation of pDNA/chitosan/sugar–PEG-A/C ternary complexes. (B) Structure of sugar–PEG-A/Cs.

10300. A pDNA/chitosan complex was prepared according to the method previously reported.[3] The P/N ratio, which is the ratio of phosphate anion (P) of pDNA to the amino group (N) of chitosan, was 1/5. Ternary complexes were prepared by mixing preformed pDNA/chitosan complexes with aqueous solutions of PEG-A/C or sugar–PEG-A/Cs at appropriate P/N/C (C is carboxyl group of PEG-A/C) ratios for 15 min. In this study, pGL3-Luc (Promega) encoding the *luciferase* gene was employed as pDNA.

AFM observation with SPM-300 (Seiko Instruments Inc., Japan) indicated that the pDNA/chitosan complexes (P/N > 3) showed spherical structures of 200 nm in diameter. The morphology and size of the pDNA/chitosan/PEG-A/C complex at P/N/C = 1/5/20 were similar to the pDNA/chitosan complex. The particle size of the pDNA/chitosan/sugar–PEG-A/C complex was about 500 nm at N/P/C = 1/5/10 and 1/5/20. There was no obvious morphological difference between the pDNA/chitosan/Mal–PEG-A/C and pDNA/chitosan/Lac–PEG-A/C complexes.

The zeta potential was determined at various P/N/C ratios of the ternary complexes with a ZeeCom (Microtec Co., Ltd., Japan) at 25 °C (Figure 2). The zeta potential of the pDNA/chitosan complex at P/N = 1/5 was +49 mV, and was decreased by coating it with sugar–PEG-A/Cs. The zeta potentials of the pDNA/chitosan/sugar–PEG-A/C complexes were negative at P/N/C = 1/5/10 and 1/5/20. Therefore, it is considered that the surface of the cationic pDNA/chitosan complex was coated with anionic Mal–PEG-A/C and Lac–PEG-A/C.

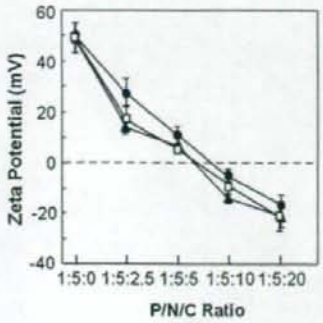

Figure 2. Zeta potentials of pDNA/chitosan/PEG-A/C (closed triangle), pDNA/chitosan/Mal–PEG-A/C (open square), and pDNA/chitosan/Lac–PEG-A/C (closed circle) complexes in 20 mM HEPES buffer. [pDNA] = 1.5 μg/mL.

The resistance of ternary complexes to degradation by DNaseI was investigated by agarose gel electrophoresis. The naked pDNA was completely digested by DNaseI (0.1 U) 50 mM Tris-HCl buffer containing 10 mM $MgCl_2$ and 100 mM NaCl at 37 °C for 30 min. On the other hand, the pDNA/chitosan and pDNA/chitosan/sugar–PEG-A/C complexes showed markedly improved resistance against DNaseI.

Luciferase activities of pDNA/chitosan/PEG-A/C complexes were investigated for B16 mouse melanoma cells. The transfection efficiency of the pDNA/chitosan/PEG-A/C complex at P/N/C = 1/5/2.5 decreased to one tenth that of the pDNA/chitosan complex. The transfection efficiencies of the ternary complexes were recovered by increasing the amount of PEG-A/C, and that of the complex of P/N/C = 1/5/40 was almost comparable with that of the pDNA/chitosan complex.

Next, the transfection efficiencies of the pDNA/chitosan/sugar–PEG-A/C complexes were investigated for B16 cells (Figure 3). The transfection efficiencies of pDNA/chitosan/

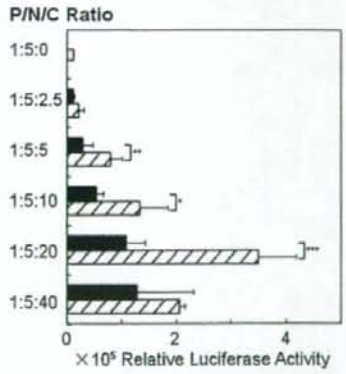

Figure 3. Transfection efficiencies of pDNA/chitosan/Lac–PEG-A/C (black bar) and pDNA/chitosan/Mal–PEG-A/C (cross-hatched bar) complexes at different P/N/C ratios. The luciferase activity of naked pDNA was normalized to 100. The luciferase activity of B16 cells transfected with 2.5 μg of pDNA per 2×10^5 cells represents the mean values of three experiments. The transfection time was 4 h, and post-transfection time was 20 h. * $P < 0.1$, ** $P < 0.05$, *** $P < 0.01$.

Lac–PEG-A/C and pDNA/chitosan/Mal–PEG-A/C complexes at P/N/C = 1/5/20 were 5.5- and 20-fold higher, respectively, than that of the pDNA/chitosan complex. The increased transfection efficiencies of the pDNA/chitosan/sugar–PEG-A/C complexes were also observed for human hepatoma HepG2 cells.

Since both the pDNA/chitosan/Lac–PEG-A/C and pDNA/chitosan/Mal–PEG-A/C complexes showed enhanced transfection efficiencies compared with pDNA/chitosan complexes, it was considered that physicochemical stability contributed to their high transfection efficiency. Thus, the interactions of the DNA complexes with anionic serum albumin and glycosaminoglycan (chondroitin sulfate) were investigated. The turbidity (at 350 nm) of the pDNA/chitosan complex markedly increased depending on the concentration of BSA (0.1–1 mg/mL), whereas those of the pDNA/chitosan/Mal–PEG-A/C complexes were significantly suppressed. Furthermore, the release of pDNA from the pDNA/chitosan and pDNA/chitosan/Mal–PEG-A/C complexes in the presence of 2% chondroitin sulfate was investigated by agarose gel electrophoresis. Though pDNA was released from the pDNA/chitosan complex, no release was observed from the pDNA/chitosan/Mal–PEG-A/C complex. These results suggested that the stability of the pDNA/chitosan complex against polyanions was improved by coating its surface with sugar–PEG-A/Cs. Improvement of the physicochemical stability of chitosan-containing gene carriers would be preferable for in vivo administration.

This work was partly supported by the Special Coordination of Funds for Promoting Science and Technology from the Ministry of Education, Culture, Sports, Science and Technology, Japan (T. S.).

References and Notes

1 S. Hirano, H. Seino, Y. Akiyama, I. Nonaka, *Polym. Eng. Sci.* **1988**, *59*, 897.
2 T. Sato, N. Shirakawa, H. Nishi, Y. Okahata, *Chem. Lett.* **1996**, 725.
3 a) T. Ishii, Y. Okahata, T. Sato, *Biochim. Biophys. Acta* **2001**, *1514*, 51. b) T. Sato, T. Ishii, Y. Okahata, *Biomaterials* **2001**, *22*, 2075.
4 a) K. Roy, H.-Q. Mao, S.-K. Huang, K. W. Leong, *Nature Med.* **1999**, *5*, 387. b) L. Illum, I. Jabbal-Gill, M. Hinchcliffe, A. N. Fisher, S. S. Davis, *Adv. Drug Delivery Rev.* **2001**, *51*, 81.
5 a) M. Hashimoto, M. Morimoto, H. Saimoto, Y. Shigemasa, T. Sato, *Bioconjugate Chem.* **2006**, *17*, 309. b) M. Hashimoto, M. Morimoto, H. Saimoto, Y. Shigemasa, H. Yanagie, M. Eriguchi, T. Sato, *Biotech. Lett.* **2006**, *28*, 815.
6 M. Ogris, S. Brunner, S. Schüller, R. Kircheis, E. Wagner, *Gene Ther.* **1999**, *6*, 595.
7 a) H.-Q. Mao, K. Roy, V. L. Troung-Le, K. A. Janes, K. Y. Lin, Y. Wang, J. T. August, K. W. Leong, *J. Controlled Release* **2001**, *70*, 399. b) I. K. Park, T. H. Kim, Y. H. Park, B. A. Shin, E. S. Choi, E. H. Chowdhury, T. Akaike, C. S. Cho, *J. Controlled Release* **2001**, *76*, 349.
8 Y. Koyama, E. Yamada, T. Ito, Y. Miautani, T. Yamaoka, *Macromol. Biosci.* **2002**, *2*, 251.
9 S. M. Moghimi, P. Symonds, J. C. Murray, A. C. Hunter, G. Debska, A. Szewczyk, *Mol. Ther.* **2005**, *11*, 990.
10 M. Köping-Höggård, I. Tubulekas, H. Guan, K. Edwards, M. Nilsson, K. M. Vårum, P. Artursson, *Gene Ther.* **2001**, *8*, 1108.
11 Supporting Information is available electronically on the CSJ-Journal Web site, http://www.csj.jp/journals/chem-lett.

Published on the web (Advance View) February 2, 2008; doi:10.1246/cl.2008.266

Available online at www.sciencedirect.com
ScienceDirect
Carbohydrate Research 343 (2008) 831–838
Carbohydrate RESEARCH

Glycosylation of dodecyl 2-acetamido-2-deoxy-β-D-glucopyranoside and dodecyl β-D-galactopyranosyl-(1→4)-2-acetamido-2-deoxy-β-D-glucopyranoside as saccharide primers in cells

Toshinori Sato,[a,*] Minako Takashiba,[a] Rumi Hayashi,[a] Xingyu Zhu[a] and Tatsuya Yamagata[b]

[a]*Department of Biosciences and Informatics, Keio University, Yokohama 223-8522, Japan*
[b]*Shenyang Pharmaceutical University, PO Box 29, School of Pharmaceutical Engineering, Shenyang 110016, PR China*

Received 3 July 2007; received in revised form 26 December 2007; accepted 16 January 2008
Available online 26 January 2008

Abstract—Syntheses of oligosaccharides expressed on cells are indispensable for the improvement of the functional analyses of the oligosaccharides and their applications. We are developing saccharide primers for synthesizing oligosaccharides using living cells. In this study, dodecyl 2-acetamido-2-deoxy-β-D-glucopyranoside (GlcNAc-C12) and dodecyl β-D-galactopyranosyl-(1→4)-2-acetamido-2-deoxy-β-D-glucopyranoside (LacNAc-C12) were examined for their abilities to prime the syntheses of neolacto-series oligosaccharides in HL60 cells. When GlcNAc-C12 was incubated with HL60 cells in serum-free medium for 2 days, 14 kinds of glycosylated products were collected from the culture medium. They were separated by high-performance liquid chromatography. The sequences of the products were determined to be neolacto-series oligosaccharides including Lewis^X, sialyl Lewis^X, polylactosamine, and sialylpolylactosamine by mass spectrometry. GlcNAc-C12 was also glycosylated by B16 cells and gave sialyllactosamine. Furthermore, LacNAc-C12 gave similar glycosylated products to GlcNAc-C12.

Keywords: Saccharide primer; *N*-Acetylglucosamine; *N*-Acetyllactosamine; Oligosaccharide; Glycosylation; Animal cells

1. Introduction

The importance of technology to synthesize oligosaccharides expressed on mammalian cells has been indicated by the elucidation of their roles in cell function. We have been developing saccharide primer methods to synthesize oligosaccharides using the glycan biosynthesis system in cells. A saccharide primer is a glycolipid analogue to be glycosylated by cells in culture. Yamagata and co-workers have developed amphiphilic glycolipid analogues such as alkyllactosides.[1,2] Dodecyl β-lactoside (Lac-C12) as a saccharide primer was incorporated into B16 melanoma cells and was glycosylated by glycosyltransferase. The glycosylated product was secreted from the cells. Structural analyses indicated that the product was sialyllactose, which is the carbohydrate portion of GM3 normally expressed on the surface of mouse B16 melanoma cells.

Other primers as substrates for glycosyltransferase in cells have been described in several reports. β-D-Xylosides have been developed as an initiator of glycosaminoglycan biosynthesis.[3,4] Acetylated Xylβ1-6Gal-*O*-2-naphthol and acetylated Galβ1-4GlcNAcβ-*O*-naphthalenemethanol (NM) were investigated as inhibitors of the glycosyltransferase in cells.[5] Furthermore, acetylated Galβ1-4GlcNAcβ-NM and acetylated GlcNAcβ1-3Galβ-NM inhibited the biosynthesis of endogenous sialyl Lewis^X, and they were also glycosylated in human promyelocytic leukemia HL60 cells.[6]

The glycosylation of the saccharide primers was suggested to be dependent on the cell lines, because different types of cells have different intrinsic glycan biosynthesis

* Corresponding author. Tel.: +81 45 566 1771; fax: +81 45 566 1447; e-mail: sato@bio.keio.ac.jp

0008-6215/$ - see front matter © 2008 Elsevier Ltd. All rights reserved.
doi:10.1016/j.carres.2008.01.022

systems. Therefore, a saccharide library could be synthesized by combining various saccharide primers and cells. HL60 cells are known to express ganglioside GM3 and neolacto-series oligosaccharides. When Lac-C12 was incubated with HL60 cells, only the sialylated product (sialyllactose) was obtained, but not neolacto-series oligosaccharides. Therefore, in the present study, we synthesized dodecyl 2-acetamido-2-deoxy-β-D-glucopyranoside (GlcNAc-C12) and dodecyl β-D-galactopyranosyl-(1→4)-2-acetamido-2-deoxy-β-D-glucopyranoside (LacNAc-C12) as saccharide primers (Fig. 1), and the glycosylation reactions of those primers by HL 60 cells and B16 cells were examined.

2. Results

2.1. Glycosylation of GlcNAc-C12 by HL60 cells

HL60 cells were employed to examine the usefulness of GlcNAc-C12 as saccharide primer for the synthesis of neolacto-series oligosaccharides. After incubation of 50 μM of GlcNAc-C12 with HL60 cells, glycosylated products and unreacted primers were collected from the culture medium and cell fraction using a Sep-Pak C_{18} column. The glycosylated products adsorbed to the column were eluted using mixed solvents of methanol and water. The glycosylated products were largely detected from the culture medium. The acidic and neutral products were eluted with 3:7 MeOH–H_2O, and 1:9 MeOH–H_2O, respectively. As shown in Figure 2A, HPTLC (high-performance thin-layer chromatography) indicated that the fractions eluted with 3:7 MeOH–H_2O contained four neutral products (N1–N4), and the fractions eluted with 1:9 MeOH–H_2O contained six acidic products (A1–A6). Next, the neutral and acidic products were separated by high-performance liquid chromatography (HPLC). The four neutral products were separated using 70:28:2 $CHCl_3$–MeOH–H_2O as shown in Figure 2B. N1, N2, N3, and N4 were detected in fraction numbers 7–9, 11–12, 35–40, and 70–80, respectively. The four acidic products (A1–A4) were separated using 70:28:2 $CHCl_3$–MeOH–H_2O as shown in Figure 2C. A1, A2, A3, and A4 were detected in fraction numbers 17–19, 20–23, 26–28, and 45–50, respectively. Two acidic products (A5–A6) were separated using 60:35:5 $CHCl_3$–MeOH–H_2O as shown in Figure 2D. A4 and A5 were detected in fraction numbers 10 and 11–13, respectively.

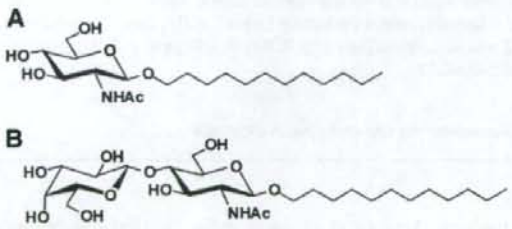

Figure 1. Saccharide primers, GlcNAc-C12 (A) and LacNAc-C12 (B), employed in this study.

2.2. Analyses of the chemical structures of products by mass spectrometry

Analyses of the structures of products separated by HPLC were carried out by MALDI-TOFMS (matrix-assisted laser desorption and ionization time-of-flight mass spectrometry). The observed masses and the deduced sequences of the glycosylated products are shown in Table 1. The mobility of N1 on HPTLC was same as that of synthetic Galβ1-4GlcNAc-C12 (LacNAc-C12), and the non-reducing hexose of N1 was cleaved by jack bean β-galactosidase (data not shown). Furthermore, the positive MALDI-PSD (post-source decay)

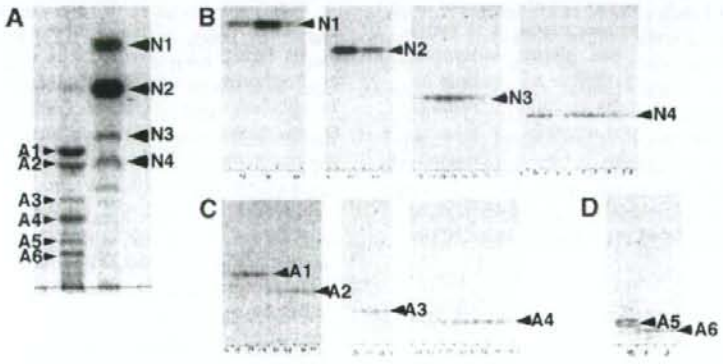

Figure 2. HPTLC of the products collected using a Sep-Pak C_{18} column (A), and purified by HPLC (B, C, and D) for the glycosylation of GlcNAc-C12 by HL60 cells.

Table 1. Deduced sequences and mass observed by MALDI-TOF-MS for the glycosylated products from GlcNAc-C12

Product	Sequence	Observed mass
N1	Galβ1-4GlcNAc-C12	574.1 $[M+Na]^+$
N2	Galβ1-4(Fucα1-3)-GlcNAc-C12	720.1 $[M+Na]^+$
N3	Galβ1-4GlcNAcβ1-3Galβ1-4GlcNAc-C12	939.1 $[M+Na]^+$
N4	Galβ1-4GlcNAcβ1-3Galβ1-4(Fucα1-3)GlcNAc-C12	1085.3 $[M+Na]^+$
A1	NeuNAcα2-3Galβ1-4GlcNAc-C12	841.4 $[M-H]^-$
A2	NeuNAcα2-6Galβ1-4GlcNAc-C12	841.4 $[M-H]^-$
A3	NeuNAc-(Galβ1-4GlcNAc)$_2$-C12	1230.1 $[M-H]^-$
A4	Fucose+A3	1376.3 $[M-H]^-$
A5	NeuNAc-(Galβ1-4GlcNAc)$_3$-C12	1595.9 $[M-H]^-$
A6	Fucose+A5	1742.0 $[M-H]^-$

spectrum (Table 2) revealed a peak at m/z 305.32 corresponding to $^{0,2}A_2$ fragment ($+Na^+$, intramolecular cleavage of GlcNAc). The results of MALDI-PSD agreed with the values in the literature.[7] Thus, N1 was determined to be Galβ1-4GlcNAc-C12. N2 was predicted to be H antigen (Fuc-Gal-GlcNAc-C12) or Lewis^X (Gal-(Fuc)-GlcNAc-C12) from the peak of m/z 720.1 ($[M+Na]^+$) of the MALDI-TOF-MS spectrum (Table 1). The MALDI-PSD spectrum of N2 (Table 2) revealed peaks at m/z 558.4 corresponding to $Y_{1\beta}$ (Fuc-GlcNAc-C12+Na^+) and m/z 305.4 corresponding to the $Y_{1\alpha}/^{0,2}A_2$ fragment ($+Na^+$). The observed fragment ions of N2 were similar to the MALDI-PSD spectrum of Lewis^X reported in the literature.[7] Therefore, N2 was determined to be Lewis^X. N3 was predicted to be Gal-GlcNAc-Gal-GlcNAc-C12 from the peak of m/z 939.1 ($[M+Na]^+$) of the MALDI-TOF-MS spectrum (Table 1). The MALDI-PSD spectrum of N3 (Table 2) revealed peaks at m/z 670.5 corresponding to $^{0,2}A_4$ fragment ($+Na^+$) and m/z 305.3 corresponding to $^{0,2}A_2$ fragment ($+Na^+$), suggesting the existence of two β-(1→4) lactosamine units. N4 was predicted to be fucosylated N3 from the peak of m/z 1085.3 ($[M+Na]^+$) of the MALDI-TOF-MS spectrum (Table 1). The MALDI-PSD spectrum of N4 (Table 2) revealed a peak at m/z 558.6 corresponding to $Y_{1\beta}$ (Fuc-GlcNAc-C12+Na^+), and fragmentation ions were similar to those of N3, suggesting that N4 is Galβ1-4GlcNAcβ1-3Galβ1-4(Fucα1-3)GlcNAc-C12. HL60 cells express FUT4, which transfers fucose to lactosamine.[8] Furthermore, it has been reported that FUT4 preferentially transfers fucose to inner GlcNAc residues.[9] The structure of N5 agreed with that of the endogenous glycan reported in the literature.[8,9]

Though the mobilities of A1 and A2 on HPTLC were different, the MALDI-TOF-MS spectra of them revealed the same mass of 841.4 ($[M-H]^-$), corresponding to NeuNAc-Gal-GlcNAc-C12 (sLacNAc-C12, Table 1). Since A1 and A2 are considered to have different linkages of *N*-acetylneuraminic acid to galactose, the

Table 2. Fragment ions observed by MALDI-PSD spectrum for the glycosylated products from GlcNAc-C12

Product	Fragments
N1	226.4 ($[Y_1/B_2+Na]^+$), 305.3 ($[^{0,2}A_2+Na]^+$), 388.4 ($[B_2+Na]^+$), 412.4 ($[Y_1+Na]^+$),
N2	226.3 ($[Y_{1\alpha}/Y_{1\beta}/B_2+Na]^+$), 305.4 ($[Y_{1\alpha}/^{0,2}A_2+Na]^+$), 370.5 ($[Z_1/B_2+Na]^+$), 388.3 ($[Y_{1\alpha}/B_2+Na]^+$), 412.4 ($[Y_{1\alpha}/Y_{1\beta}+Na]^+$), 534.4 ($[B_2+Na]^+$), 556.4 ($[Z_1+Na]^+$), 558.4 ($[Y_{1\beta}+Na]^+$), 574.6 ($[Y_{1\alpha}+Na]^+$)
N3	226.3 ($[Y_3/B_2+Na]^+$, $[B_4/Y_1+Na]^+$), 305.3 ($[^{0,2}A_2+Na]^+$), 388.2 ($[B_2+Na]^+$ or $[B_4/Y_2+Na]^+$), 406.4 ($[C_2+Na]^+$), 412.5 ($[Y_1+Na]^+$), 550.3 ($[B_3+Na]^+$), 574.5 ($[Y_2+Na]^+$), 670.5 ($[^{0,2}A_4+Na]^+$), 753.7 ($[B_4+Na]^+$), 777.9 ($[Y_3+Na]^+$)
N4	226.4 ($[Y_3/B_2+Na]^+$, $[Y_{1\alpha}/B_4/Y_{1\beta}+Na]^+$), 305.3 ($[^{0,2}A_2+Na]^+$), 388.5 ($[B_2+Na]^+$ or $[Y_{1\alpha}/B_4/Y_2+Na]^+$), 406.5 ($[C_2+Na]^+$), 412.7 ($[Y_{1\alpha}/Y_{1\beta}+Na]^+$), 550.6 ($[B_3+Na]^+$), 558.7 ($[Y_{1\beta}+Na]^+$), 574.9 ($[Y_{1\alpha}/Y_2+Na]^+$), 670.4 ($[Y_{1\alpha}/^{0,2}A_4+Na]^+$), 720.6 ($[Y_2+Na]^+$), 778.0 ($[Y_{1\alpha}/Y_3+Na]^+$), 901.9 ($[Y_3+Na]^+$), 940.0 ($[Y_{1\alpha}+Na]^+$)
A3	388.3 ($[Y_4/B_3+Na]^+$, $[Y_2/B_5+Na]^+$), 406.5 ($[Y_4/C_3+Na]^+$), 412.4 ($[Y_1+Na]^+$), 476.3 ($[B_2+Na]^+$), 550.5 ($[Y_4/B_4+Na]^+$), 574.6 ($[Y_2+Na]^+$), 634.9 ($[^{0,2}A_3+Na+K-H]^+$), 679.6 ($[B_7+Na]^+$), 753.8 ($[B_5/Y_3+Na]^+$), 777.7 ($[Y_3+Na]^+$), 939.8 ($[Y_4+Na]^+$)
A4	336.4 ($[B_1+2Na-H]^+$), 388.4 ($[Y_4/B_3+Na]^+$ or $[Y_{1\alpha}/Y_2/B_5+Na]^+$), 406.5 ($[Y_4/C_3+Na]^+$), 412.3 ($[Y_{1\alpha}/Y_{1\beta}+Na]^+$), 476.5 ($[B_2+Na]^+$), 550.6 ($[Y_4/B_4+Na]^+$), 558.9 ($[Y_{1\beta}+Na]^+$), 574.6 ($[Y_{1\alpha}/Y_2+Na]^+$), 634.9 ($[^{0,2}A_3+Na+K-H]^+$), 679.6 ($[B_3+Na]^+$), 720.9 ($[Y_2+Na]^+$), 777.8 ($[Y_{1\alpha}/Y_3+Na]^+$), 841.3 ($[B_4+Na]^+$), 923.9 ($[Y_3+Na]^+$), 939.6 ($[Y_{1\alpha}/Y_4+Na]^+$), 1085.4 ($[Y_4+Na]^+$), 1230.8 ($Y_{1\alpha}$)
A5	388.1 ($[Y_6/B_3+Na]^+$, $[B_5/Y_4+Na]^+$ or $[B_7/Y_2+Na]^+$), 406.2 ($[Y_6/C_3+Na]^+$ or $[C_5/Y_4+Na]^+$), 550.3 ($[B_6/Y_4+Na]^+$), 574.6 ($[Y_2+Na]^+$), 591.2 ($[Y_5/B_5+Na]^+$ or $[B_7/Y_4+Na]^+$), 596.7 ($[^{0,2}A_3+Na]^+$), 634.9 ($[^{0,2}A_3+Na+K-H]^+$), 670.2 ($[Y_6/^{0,2}A_5+Na]^+$, $[Y_4/^{0,2}A_7+Na]^+$), 679.5 ($[B_3+Na]^+$), 753.6 ($[Y_6/B_5+Na]^+$ or $[B_7/Y_4+Na]^+$), 777.6 ($[Y_3+Na]^+$), 916.8 ($[Y_4+H]^+$), 939.5 ($[Y_4+Na]^+$), 999.8 ($[^{0,2}A_5+Na]^+$), 1045.1 ($[B_5+Na]^+$), 1142.7 ($[Y_5+Na]^+$), 1305.0 ($[Y_6+Na]^+$)
A6	388.6 ($[Y_6/B_3+Na]^+$, $[B_5/Y_4+Na]^+$ or $[Y_{1\alpha}/B_7/Y_2+Na]^+$), 406.8 ($[Y_6/C_3+Na]^+$, $[C_5/Y_4+Na]^+$), 550.5 ($[B_6/Y_4+Na]^+$), 574.9 ($[Y_{1\alpha}/Y_2+Na]^+$), 591.3 ($[Y_5/B_5+Na]^+$ or $[Y_{1\alpha}/B_7/Y_3+Na]^+$), 596.2 ($[^{0,2}A_3+Na]^+$), 634.4 ($[^{0,2}A_3+Na+K+H]^+$), 720.2 ($[Y_2+Na]^+$), 753.8 ($[Y_{1\alpha}/Y_6/^{0,2}A_5+Na]^+$ or $[Y_{1\alpha}/Y_4/^{0,2}A_7+Na]^+$), 777.6 ($[Y_{1\alpha}/Y_3+Na]^+$), 899.9 ($[Y_4/B_7+Na]^+$), 916.9 ($[Y_{1\alpha}/Y_4+H]^+$), 923.9 ($[Y_3+Na]^+$), 939.8 ($[Y_{1\alpha}/Y_3+Na]^+$), 1000.0 ($[Y_{1\alpha}/^{0,2}A_5+Na]^+$), 1045.5 ($[B_5+Na]^+$), 1085.7 ($[Y_4+Na]^+$), 1288.8 ($[Y_5+Na]^+$), 1304.5 ($[Y_{1\alpha}/Y_6+Na]^+$), 1451.0 ($[Y_6+Na]^+$), 1472.6 ($[Y_6+2Na-H]^+$), 1596.1 ($[Y_{1\alpha}+Na]^+$)

enzymatic cleavages of sLacNAc-C12 by neuraminidases were examined. The neuraminidases employed in this study were *Arthrobacter ureafacience* neuraminidase, which hydrolyzes α-(2→3), α-(2→6), and α-(2→8) linkages,[10] and *Macrobdella decora* neuraminidase, which hydrolyzes α-(2→3) linkage.[11] Though *N*-acetylneuraminic acid of A1 was cleaved by both neuraminidases, that of A2 was cleaved by the *A. ureafacience* neuraminidase but not by the *M. decora* neuraminidase. The hydrolyzed products showed the same mobility as synthetic Galβ1-4GlcNAc-C12. Next, ESI (electrospray ionization)-CID (collision-induced dissociation) was employed to distinguish between A1 and A2. The ESI-CID spectra of A1 and A2 showed peaks of *m/z* 887.5 ($[M+2Na-H]^+$) corresponding to NeuNAc-Gal-GlcNAc-C12, and *m/z* 574.3 ($[(M\text{-anNeuNAc})+Na]^+$) corresponding to Y_2 fragment (Gal-GlcNAc-C12). The relative intensity of Y_2 (*m/z* 574.3) to the parent peak (*m/z* 887.5) showed significant differences between A1 and A2, and was 0.68 for A1 and 0.03 for A2. It has been reported that α-(2→3) sialyl linkage was distinguished from α-(2→6) sialyl linkage based on the ESI-CID spectra.[12] In the literature, the fragmentation ions produced by the cleavage of the α-(2→3) sialyl linkage showed much higher intensity than those produced by the cleavage of the α-(2→6) sialyl linkage. Therefore, from the results of enzymatic digestions and ESI-CID spectra, A1 and A2 were determined to be NeuNAcα2-3Galβ1-4GalNAc-C12 and NeuNAcα2-6Galβ1-4GalNAc-C12, respectively.

The MALDI-TOFMS spectra of A3 and A5 (Table 1) revealed peaks of *m/z* 1230.1 ($[M-H]^-$) corresponding to NeuNAc-(Gal-GlcNAc)$_2$-C12 and *m/z* 1571.7 ($[M-H]^-$) corresponding to NeuNAc-(Gal-GlcNAc)$_3$-C12. A3 was considered to be produced by the sialylation of N4. The MALDI-TOF-MS spectra of A4 and A6 revealed peaks of *m/z* 1352.7 ($[M-H]^-$) corresponding to fucosylated A3 and *m/z* 1779.0 ($[M-H]^-$) corresponding to fucosylated A5. The positive-ion mode MALDI-PSD spectrum of A4 (Table 2) revealed peaks at *m/z* 558.9 corresponding to $Y_{1\beta}$ (Fuc-GlcNAc-C12+Na^+) and *m/z* 720.9 corresponding to Y_2 (Fuc+Gal-GlcNAc-C12+Na^+). The positive-ion mode MALDI-PSD spectrum of A6 (Table 2) also revealed a peak at *m/z* 720.2 corresponding to Y_2 (Fuc+Gal-GlcNAc-C12+Na^+), *m/z* 923.9 corresponding to Y_3 (Fuc+GlcNAc-Gal-GlcNAc-C12+Na^+), and *m/z* 1085.7 corresponding to Y_4 (Fuc+Gal-GlcNAc-Gal-GlcNAc-C12+Na^+). These MALDI-PSD spectra suggested that the fucose moieties in A4 and A6 were linked to the innermost GlcNAc residue. It has been reported that HL60 cells express α-(1→3)-fucosyltransferase, and fucosylated monosialyl glycolipids having similar structures to A4 and A6 were detected in HL60 cells.[13] Though the linkages of *N*-acetylneuraminic acid in A3, A4, A5, and A6 could not be determined in the present study, they were inferred to be α-(2→3) from the structural analysis of the sialyl linkage of sialylpolylactosamine expressed in HL60 cells.[14]

2.3. Glycosylation of LacNAc-C12 by HL60 cells

Next, the glycosylation of LacNAc-C12 by HL60 cells was examined. After incubation of HL60 cells with 50 μM LacNAc-C12 for 2 days, glycosylated products and unreacted primer were isolated from the culture medium. The glycosylated products collected using a Sep-Pak C_{18} column were analyzed by HPTLC. One neutral product and six acidic products were detected. The analyses of mobility on HPTLC and the mass spectrum indicated that the products glycosylated from LacNAc-C12 were the same as those from GlcNAc-C12. The neutral product was N2 and the acidic products were A1–A6.

2.4. Comparison of GlcNAc-C12 and LacNAc-C12 as glycosyl acceptors in B16 cells

After incubation of 50 μM GlcNAc-C12 or LacNAc-C12 with B16 cells for 2 days, glycosylated products were isolated from the culture medium. The glycosylated products were analyzed by HPTLC and MALDT-TOF-MS. Using GlcNAc-C12, two glycosylated products were detected. One was Gal-GlcNAc-C12, whose mobility on HPTLC was the same as that of synthetic LacNAc-C12. The other was considered to be NeuNAc-Gal-GlcNAc-C12 (sLacNAc-C12) from the mass spectrum. For LacNAc-C12, the detected product was also suggested to be sLacNAc-C12 from the mobility on HPTLC and from the mass spectrum. To determine the linkage of the sialic acid, the product was treated with neuraminidases from *A. ureafaciens* and *M. decora*. Since the glycosylated product sLacNAc-C12 was hydrolyzed by both sialidases, the linkage of NeuNAc-Gal was determined to be α-(2→3). The amount of sLacNAc-C12 derived from GlcNAc-C12 was two times higher than that from LacNAc-C12, when the dose of saccharide primers was 50 μM (Fig. 3). The glycosylation efficiency of GlcNAc-C12 in cells was higher than that of LacNAc-C12 in cells. When the dose of GlcNAc-C12 was 50 μM (250 nmol), the amount of sLacNAc-C12 was determined to be 7.5 nmol by quantitative analysis using GM1 as standard.

2.5. Cell growth in the presence of saccharide primers

B16 cells were cultured in the absence and the presence of 50 μM GlcNAc-C12 and LacNAc-C12 for 2 days. The cell growth in the presence of the saccharide primers was almost similar to that of control (Fig. 4). Cell growth of HL60 cells was also investigated in the presence of 50 μM GlcNAc-C12 for 2 days (data not

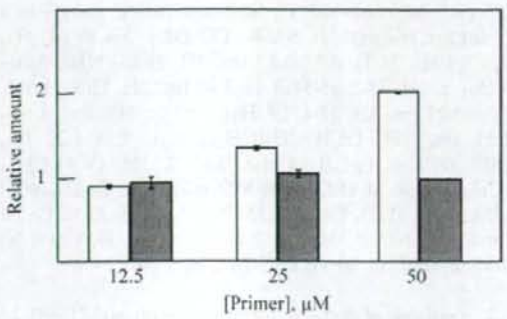

Figure 3. Relative amounts of NeuNAc-Gal-GlcNAc-C12 glycosylated from GlcNAc-C12 (white column) and Gal-GlcNAc-C12 (black column) by B16 melanoma cells (2×10^6 cells). The relative amounts were analyzed by densitometry at 540 nm followed by staining with resorcinol–HCl. The dose of saccharide primers was 50 μM.

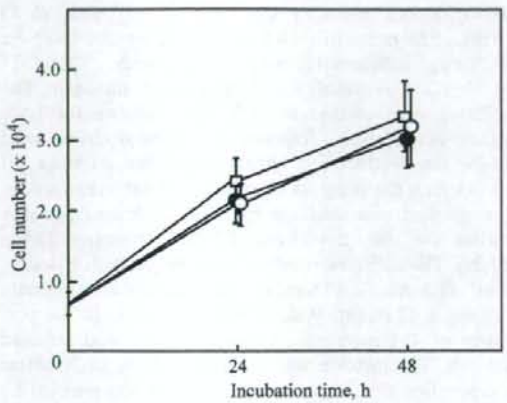

Figure 4. Growth of B16 cells cultured in the absence (closed circle) and the presence of 50 μM GlcNAc-C12 (open circle) and LacNAc-C12 (open square).

shown). The primers showed no cytotoxicity at the present experimental conditions.

3. Discussion

Convenient synthesis of glycan structures present on cells is important for the study to elucidate glycan function. Since saccharide primers can act as substrates for glycosyltransferases present in cells, they are useful for the synthesis of oligosaccharides expressed in cells. Saccharide primers are building blocks for constructing an oligosaccharide library by biocombinatorial synthesis that is combination of different saccharide primers and a variety of cells. It has been reported that Lac-C12, which is a mimicry of lactosylceramide, was useful to synthesize the oligosaccharides of glycosphingolipids (GSL). For example, Lac-C12 gave GM3 oligosaccharide when incubated with B16 melanoma cells. Furthermore, 12-azido dodecyl-β-lactoside (Lac-C12-N3) was synthesized with the aim of preparing glycan arrays or glycopolymers. Lac-C12-N3 was also glycosylated by cells as well as Lac-C12[15] and could be conjugated to solid supports by the modified Staudinger reaction or condensation reaction followed by reduction to the amino group for detecting carbohydrate recognition.[16]

For the construction of oligosaccharide libraries, it is important to synthesize various oligosaccharides. In our ongoing studies, it has been found that Lac-C12 gave rise to various oligosaccharides of ganglio- and globo-series gangliosides. Then, in the present study, we synthesized novel saccharide primers to selectively obtain neolacto-series oligosaccharides. In the biosynthesis of neolacto-series glycans, the lactosamine unit of Galβ1-4GlcNAc is the precursor region for sugar elongation. Thus, saccharide primers containing GlcNAc and LacNAc would be substrates for glycosyltransferases synthesizing neolacto-series oligosaccharides. In the literature, Esko and co-workers have reported that disaccharide primers such as peracetylated Galβ1-4GlcNAc-NM were fucosylated to Galβ1-4(Fucα1-3)GlcNAc-NM, and peracetylated GlcNAcβ1-3Gal-NM was converted to Galβ1-4(Fucα1-3)GlcNAcβ1-3Gal-NM, NeuNAcα2-3Galβ1-4GlcNAcβ1-3Gal-NM, and NeuNAcα2-3Galβ1-4(Fucα1-3)GlcNAcβ1-3Gal-NM by U937 human histiocytic lymphoma cells.[6] Those peracetylated primers were glycosylated after deacetylation in cells. In our study, deacetylated saccharide primer was used for the synthesis of oligosaccharides by cells. GlcNAc-C12 and LacNAc-C12 gave Le^x, sLe^x, polylactosamine, sialylated polylactosamine, and sialylated/fucosylated polylactosamine by incubating with HL60 cells. These oligosaccharides were similar to endogenous glycans observed in HL60.[17] The complex glycosylated products were clearly separated by HPLC, and their chemical structures were determined by enzymatic digestion and mass spectrometry. Separation and structural elucidation of the products were very convenient compared to the endogenous GSLs because the saccharide primers had a uniform aglycon structure.

Since GlcNAc-C12 gave similar glycosylated products to LacNAc-C12, we could conclude that monosaccharide primers as well as disaccharide primers are useful for the synthesis of oligosaccharides. It has been reported that the glycosylation efficiencies of saccharide primers were dependent on their hydrophilic–hydrophobic balance.[2,18] More hydrophilic saccharide primers cannot be internalized into cells, while more hydrophobic ones are strongly adsorbed to the cell membrane. Although the glycosylation efficiency of GlcNAc-C12 was higher than that of LacNAc-C12 in the present study, the structure for giving optimum glycosylation

efficiency would be determined by varying the hydrocarbon chain length.

In conclusion, saccharide primers such as GlcNAc-C12 and LacNAc-C12 were developed to synthesize neolacto-series oligosaccharides using mammalian cells. The glycosylated products were separated by HPLC, and the sequences were determined by enzymatic digestion and mass spectrometry. The saccharide primers employed in this study are expected to be useful for synthesizing oligosaccharides expressed in mammalian cells.

4. Experimental

4.1. Synthesis of dodecyl 2-acetamido-2-deoxy-β-D-glucopyranoside (GlcNAc-C12)

2-Acetamido-1,3,4,6-tetra-*O*-acetyl-2-deoxy-D-glucopyranoside (Ac_4-GlcNAc) was prepared by reacting *N*-acetylglucosamine (2.5 g, 11.3 nmol, GlcNAc, Sigma) with Ac_2O (15 mL, 159 mmol, Wako Pure Chemicals) in 30 mL of pyridine according to the literature.[19] Ac_4-GlcNAc (3 g, 7.71 mmol) was mixed with TMS-OTf (4.0 mL, 21.9 mmol, E. Merck) in CH_2Cl_2 under nitrogen.[20] The solution was refluxed at 50 °C with stirring for 7 h. After evaporation followed by neutralization with Et_3N, the product was chromatographed on silica gel to examine the progress of the reaction. The reaction mixture was mixed with 1-dodecanol (3.6 mL, 15.5 mmol, Wako Pure Chemicals), $BF_3{\cdot}OEt_2$ (21 mL, 7.9 mmol, Wako Pure Chemicals) in the presence of 4 Å molecular sieves (2.5 g), and stirred at room temperature for 22 h.[21] $BF_3{\cdot}OEt$ (20.1 mL, 0.79 mmol) was added at 18 h to complete the reaction. The mixture was neutralized with Et_3N. After evaporation, the product was purified by column chromatography (Silica Gel 60, E. Merck, 7 × 30 cm, 1:1 *n*-hexane–EtOAc). Yield: 63.8% (2.53 g). ^{1}H NMR($CDCl_3$): δ 5.51 (d, 1H, $J_{2,NH}$ 8.8 Hz, NH), 5.31 (dd, 1H, $J_{2,3}$ 10.1 Hz, $J_{3,4}$ 9.5 Hz, H-3), 5.06 (dd, 1H, $J_{3,4}$ 9.5 Hz, $J_{4,5}$ 9.9 Hz, H-4), 4.65 (d, 1H, $J_{1,2}$ 8.4 Hz, H-1), 4.26 (dd, 1H, $J_{5,6b}$ 4.7 Hz, $J_{6,gem}$ 12.3 Hz, H-6a), 4.12 (dd, 1H, $J_{5,6a}$ 2.4 Hz, $J_{6,gem}$ 12.3 Hz, H-6b), 3.89–3.75 (m, 2H, $J_{2,NH}$ 8.8 Hz, $J_{1,2}$ 8.4 Hz, H-2, $OCH_2CH_2(CH_2)_9CH_3$), 3.69 (ddd, $J_{4,5}$ 9.9 Hz, $J_{5,6a}$ 2,4 Hz, $J_{5,6b}$ 4.7 Hz, H-5), 3.50–3.42 (m, 1H, $OCH_2CH_2(CH_2)_9CH_3$), 1.94, 2.02, 2.02, and 2.08 (s, each 3H, Ac), 1.60–1.50 (m, 2H, OCH_2CH_2-$(CH_2)_9CH_3$), 1.35–1.14 (m, 18H, $OCH_2CH_2(CH_2)_9CH_3$), 0.87 (t, 3H,$OCH_2CH_2(CH_2)_9CH_3$).

Dodecyl 2-acetamido-3,4,6-tri-*O*-acetyl-2-deoxy-β-D-glucopyranoside (2.5 g, 4.85 mol) in 100 mL of MeOH was deacetylated in the presence of NaOMe (270 mg, 5.0 mmol, Wako Pure Chemicals). Deprotection was carried out with stirring for 40 min. After decolorization on charcoal in EtOH, the product GlcNAc-C12 was obtained by recrystallization in ethanol. Yield: 1.70 g (88.1%). Mp 160–162 °C, lit.[22] mp 161 °C, $[\alpha]_D$ −18.8 (*c* 0.12, CH_3OH). ^{1}H NMR (CD_3OD): δ 4.38 (d, 1H, $J_{1,2}$ 6.1 Hz, H-1), 3.91–3.83 (m, 2H, H-6a, NH), 3.70–3.58 (m, 2H, H-2, H-5), 3.48–3.40 (m, 2H, H-3, H-6b), 3.34–3.27 (m, 3H, H-4, OCH_2), 1.97 (s, 3H, Ac), 1.53–1.51 (m, 2H, $OCH_2CH_2(CH_2)_9CH_3$), 1.34–1.22 (m, 18H, $OCH_2CH_2(CH_2)_9CH_3$), 0.89 (t, 3H, OCH_2CH_2-$(CH_2)_9CH_3$). MALDI-TOFMS: calcd for $C_{20}H_{39}NO_6$: $(M+Na)^+$, 412.3, Found: $(M+Na)^+$, 412.3. Anal. Calcd for $C_{20}H_{39}NO_6{\cdot}0.3H_2O$ (398.68): C, 60.82; H, 10.11; N, 3.55. Found: C, 60.81; H, 10.04; N, 3.54.

4.2. Synthesis of dodecyl β-D-galactopyranosyl-(1→4)-2-acetamido-2-deoxy-β-D-glucopyranoside (LacNAc-C12)

2,3,4,6-Tetra-*O*-acetyl-β-D-galactopyranosyl-(1→4)-2-acetamido-1,3,6-tri-*O*-acetyl-2-deoxy-β-D-glucopyranoside (Ac-LacNAc) was prepared by mixing *N*-acetyllactosamine (982 mg, 2.56 nmol, LacNAc, Yaizu Suisankagaku Industry Co. Ltd, Japan) with Ac_2O (5 mL, 52.9 mmol) in 10 mL of pyridine. Ac-LacNAc (0.799 g, 1.88 mmol) was mixed with TMS-OTf (0.24 mL, 1.33 mmol) in CH_2Cl_2 under nitrogen. The solution was refluxed at 50 °C with stirring for 12 h. After evaporation, followed by neutralization with Et_3N, the product was chromatographed on silica gel to examine the progress of reaction. After evaporation, the product was collected by column chromatography (Silica Gel 60, 2 × 23 cm, 1:2:0.01 toluene–EtOAc–Et_3N). The collected products were mixed with 1-dodecanol (1.3 mL, 5.89 mmol), (*R*,*S*)-camphor sulfonate (27 mg, 0.12 mmol, Wako Pure Chemicals) in the presence of 4 Å molecular sieves (350 mg), and refluxed for 6 h. The mixture was neutralized with Et_3N. After evaporation of the solvent, the product was purified by column chromatography (Silica Gel 60, 2 × 35 cm, 2:3 *n*-hexane–EtOAc). Yield: 50% (478 mg). ^{1}H NMR ($CDCl_3$): δ: 5.63 (d, 1H, $J_{NH,2}$ 9.3 Hz, NH), 5.35 (d, 1H, $J_{3',4'}$ 2.9 Hz, H-4′), 5.11 (dd, 1H, H-2′), 5.06 (dd, 1H, $J_{3,4}$ 8.1 Hz, H-3), 4.97 (dd, 1H, $J_{2',3'}$ 10.3 Hz, H-3′), 4.51–4.46 (m, 2H, H-1′, H-6a), 4.43 (d, 1H, $J_{1,2}$ 7.3, H-1), 4.15–4.09 (m, 3H, H-6b, H-6b′, H-6a′), 4.03 (dd, 1H, $J_{2,3}$ 9.3 Hz, H-2), 3.87 (ddd, 1H, H-5′), 3.78 (dd, 1H, H-4), 3.62 (ddd, 1H, $J_{4,5}$ 5.6 Hz, H-5), 3.41 (dd, 2H, $OCH_2CH_2(CH_2)_9CH_3$), 2.15–1.96 (m, 21H, Ac), 1.60–1.46 (m, 2H, $OCH_2CH_2(CH_2)_9CH_3$), 1.30–1.18 (m, 18H, $OCH_2CH_2(CH_2)_9CH_3$), 0.87 (t, 3H, $OCH_2(CH_2)_{10}CH_3$).

Dodecyl 2,3,4,6-tetra-*O*-acetyl-β-D-galactopyranosyl-(1→4)-2-acetamido-3,6-di-*O*-acetyl-2-deoxy-β-D-glucopyranoside (478 g, 0.56 mmol) in 25 mL of MeOH was deacetylated by the addition of NaOMe (160 mg, 2.97 mmol) with stirring for 3 h. The reactant was concentrated after treating with Amberlite IR-120B (Organo Co., Japan). LacNAc-C12 was purified by distilling with EtOH, toluene, and $CHCl_3$. Yield: 326 mg

(99%). mp 246 °C, $[\alpha]_D$ −7.6 (*c* 0.2, DMSO). ^{1}H NMR(DMSO-d_6): δ 7.74 (d, 1H, NH), 4.28 (d, 1H, $J_{1,2}$ 7.8 Hz, H-1′), 4.19 (d, 1H, $J_{1,2}$ 8.1 Hz, H-1), 1.7 (s, 3H, Ac), 1.42–1.41 (m, 2H, $OCH_2CH_2(CH_2)_9CH_3$), 1.17–1.29 (m, 18H, $OCH_2CH_2(CH_2)_9CH_3$), 0.85 (t, 3H, $OCH_2CH_2(CH_2)_9CH_3$). MALDI-TOFMS: calcd for $C_{26}H_{49}NO_{11}$: $(M+Na)^+$, 574.3, found: $(M+Na)^+$, 574.6. Anal. Calcd for $C_{26}H_{49}NO_{11}\cdot 1.5H_2O$ (578.35): C, 53.96; H, 9.06; N, 2.42. Found: C, 54.24; H, 8.77; N, 2.30.

4.3. Cell culture

HL-60 cells (Riken Cell Bank) were grown in RPMI 1640 medium (Nissui Pharm. Co., Ltd) supplemented with 10% heat-inactivated fetal bovine serum (JRH Biosciences Inc.) at 37 °C in humidified 5% CO_2. B16 cells (Riken Cell Bank) were grown in DMEM (Gibco BRL) supplemented with streptomycin 0.1 g/L, penicillin G potassium 50,000 unit/L, and 10% heat-inactivated fetal bovine serum (JRH Biosciences Inc.) at 37 °C in humidified 5% CO_2.

4.4. Glycosylation of saccharide primers in cells

Stock solutions of 20 mM saccharide primers in DMSO were diluted to 50 μM with serum-free and phenol red-free culture medium consisting of RPMI 1640 medium (Gibco BRL) containing 5 mg/L of transferrin, 5 mg/L of insulin, and 30 nM selenium dioxide.

Glycosylation by cells was carried out as follows: HL60 cells (2×10^6) were incubated with RPMI 1640 medium containing 50 μM saccharide primer for 48 h. The glycosylated products secreted in the culture medium were collected with a Sep-Pak C_{18} column (Waters Co.). The water-soluble compounds were removed with water and 3:7 MeOH–H_2O. The glycosylated products were eluted with MeOH. The eluate containing the glycosylated products was evaporated under reduced pressure. The obtained products were dissolved in 100 μL of 2:1 $CHCl_3$–MeOH, and an aliquot was separated on an HPTLC plate (Silica Gel 60, E. Merck) using $CHCl_3$–MeOH–0.2% $CaCl_2$. Acidic and neutral products on the HPTLC plate were stained with resorcinol–HCl reagent and orcinol–H_2SO_4 reagent, respectively. B16 cells (2×10^6) were similarly incubated with saccharide primers in serum-free DMEM/F-12 medium (Gibco BRL) containing 5 mg/L of transferrin, 5 mg/L of insulin, and 30 nM selenium dioxide.

4.5. TLC blotting

TLC blotting was carried out as follows: Glycosylated products separated on an HPTLC plate were sprayed with primuline reagent, and the spots were marked with a red pencil under UV light. Then, the HPTLC plate was dipped in a blotting solvent of 40:7:20 2-PrOH–MeOH–0.2% $CaCl_2$ for 20 s and placed on a glass fiber filter (ATTO Co.). The plate was covered with a PVDF membrane (ATTO Co.), a PTFE membrane (ATTO Co.), and another glass fiber filter. These layers were subjected to pressure at 180 °C for 30 s using a TLC thermal blotter (ATTO Co.). The PVDF membrane was washed with pure water, and glycolipid fractions were extracted with MeOH and 2:1 $CHCl_3$–MeOH.

4.6. High-performance liquid chromatography (HPLC)

Neutral products and acidic products separated using a Sep-Pak C_{18} column were purified by HPLC. The crude products dissolved in 70:28:2 $CHCl_3$–MeOH–H_2O were injected into an HPLC system equipped with an Iatrobead column (6RSP-8005, 4.6 × 250 mm, Iatron Laboratories Inc.) and a light scattering detector (SEDEX75, Sedere). Neutral products were separated with 70:28:2 $CHCl_3$–MeOH–H_2O. Acidic products were separated with 70:28:2 $CHCl_3$–MeOH–H_2O and 60:35:5 $CHCl_3$–MeOH–H_2O. The flow rate was 2 mL/min. The fractions were collected at 30-s intervals for 40 min.

4.7. Mass spectrometry

The structural analyses of glycosylated products were carried out by a MALDI-TOF mass spectrometer (Autoflex, Bruker Daltonics) and an ESI mass spectrometer (Esquire 3000, Bruker Daltonics). 2,5-Dihydroxybenzoic acid (DHB, Aldrich) was employed as a matrix.

4.8. Digestion of glycosylated products by enzymes

Enzymatic digestion of glycosylated products was carried out in 50 mM NaOAc buffer (pH 4.8) containing 50 mU of neuraminidase from *A. ureafaciens* (EC.3.2.1.18, Sigma), or in 50 mM sodium acetate butter (pH 5.5) containing 10 mU of neuraminidase from *M. decora* (EC. 3.2.1.18, Calbiochem). The reactions were carried out in the presence of 0.6 mg/mL sodium taurodeoxycholic acid. The products were collected using a Sep-Pak C_{18} column, separated on an HPTLC plate with 60:35:8 $CHCl_3$–MeOH–0.2% $CaCl_2$, and were stained with orcinol–H_2SO_4.

4.9. MTT assay

Cells (2×10^4) in a 96-well microplate were incubated with 50 μM GlcNAc-C12 or LacNAc-C12 for 48 h. Ten μL of WST-1 dye solution (10 mM WST-1 and 0.2 mM 1-methoxy PMS, Dojindo Laboratories) per well was added to each well. After 2 h, absorbance at 450 nm with a reference wavelength of 690 nm was measured using a microplate reader (Multiskan, Labsystem).

Acknowledgments

This work was partly supported by funds from the Program for Promotion of Basic Research Activities for Innovative Biosciences, and the Special Coordination of Funds for Promoting Science and Technology from the Ministry of Education, Culture, Sports, Science and Technology, the Japanese Government (T.S.).

Supplementary data

Supplementary data associated with this article can be found, in the online version, at doi:10.1016/j.carres.2008.01.022.

References

1. Miura, Y.; Yamagata, T. *Biochem. Biophys. Res. Commun.* **1997**, *241*, 698–703.
2. Nakajima, H.; Miura, Y.; Yamagata, T. *J. Biochem.* **1998**, *124*, 148–156.
3. Okayama, M.; Kimata, K.; Suzuki, S. *J. Biochem.* **1973**, *74*, 1069–1073.
4. Schwartz, N. B. L.; Galligani, P.-L. Ho.; Dorfman, A. *Proc. Natl. Acad. Sci. U.S.A.* **1974**, *71*, 4047–4051.
5. Sarkar, A. K.; Fritz, T. A.; Taylor, W. H.; Esko, J. D. *Proc. Natl. Acad. Sci. U.S.A.* **1995**, *92*, 3323–3327.
6. Sarkar, A. K.; Rostand, K. S.; Jain, R. K.; Matta, K. L.; Esko, J. D. *J. Biol. Chem.* **1997**, *272*, 25608–25616.
7. Yamagaki, T.; Nakanishi, H. *J. Mass Spectrom.* **2000**, *35*, 1300–1307.
8. Handa, K.; Withers, D.-A.; Hakomori, S. *Biochem. Biophys. Res. Commun.* **1998**, *243*, 199–204.
9. Nishihara, S.; Iwasaki, H.; Kaneko, M.; Tawada, A.; Ito, M.; Narimatsu, H. *FEBS Lett.* **1999**, *462*, 289–294.
10. Saito, M.; Sugano, K.; Nagai, Y. *J. Biol. Chem.* **1979**, *254*, 7845–7854.
11. Chou, M.-Y.; Li, S.-C.; Kiso, M.; Hasegawa, A.; Li, Y.-T. *J. Biol. Chem.* **1994**, *269*, 18821–18826.
12. Pan, G. G.; Melton, L. D. *J. Chromatogr.* **2005**, *1077*, 136–142.
13. Stroud, M.-R.; Holmes, E.-H. *Biochem. Biophys. Res. Commun.* **1997**, *238*, 165–168.
14. Stroud, M.-R.; Handa, K.; Salyan, M.-E.-K.; Ito, K.; Levery, S.-B.; Hakomori, S. *Biochemistry* **1996**, *35*, 758–769.
15. Kasuya, M. C. Z.; Wang, L. X.; Lee, Y. C.; Mitsuki, M.; Nakajima, H.; Miura, Y.; Sato, T.; Hatanaka, K.; Yamagata, S.; Yamagata, T. *Carbohydr. Res.* **2000**, *329*, 755–763.
16. Sato, T.; Fujita, S.; Kasuya, M. C. Z.; Hatanaka, K.; Yamagata, T. *Chem. Lett.* **2004**, *33*, 580–581.
17. Nojiri, H.; Takaku, F.; Tetsuka, T.; Motoyoshi, K.; Miura, Y.; Saito, M. *Blood* **1984**, *64*, 534–541.
18. Sato, T.; Hatanaka, K.; Hashimoto, H.; Yamagata, T. *Trends Glycosci. Glycotechnol.* **2007**, *19*, 1–17.
19. Horton, D. *J. Org. Chem.* **1964**, *29*, 1776–1782.
20. Nakabatashi, S.; Warren, C. D.; Jeanlozs, R. W. *Carbohydr. Res.* **1986**, *150*, C7–C10.
21. Xia, J.; Piskorz, C. F.; Locke, R. D.; Chandrasekaran, E. V.; Alderfer, J. L.; Matta, K. L. *Bioorg. Med. Chem. Lett.* **1999**, *9*, 2941–294622.
22. Boullanger, P.; Chevalier, Y.; Croizier, M.-C.; Lafont, D.; Sancho, M.-R. *Carbohydr. Res.* **1995**, *278*, 91–101.

Available online at www.sciencedirect.com
ScienceDirect
Carbohydrate Research 343 (2008) 831–838
Carbohydrate RESEARCH

Glycosylation of dodecyl 2-acetamido-2-deoxy-β-D-glucopyranoside and dodecyl β-D-galactopyranosyl-(1→4)-2-acetamido-2-deoxy-β-D-glucopyranoside as saccharide primers in cells

Toshinori Sato,[a,*] Minako Takashiba,[a] Rumi Hayashi,[a] Xingyu Zhu[a] and Tatsuya Yamagata[b]

[a]*Department of Biosciences and Informatics, Keio University, Yokohama 223-8522, Japan*
[b]*Shenyang Pharmaceutical University, PO Box 29, School of Pharmaceutical Engineering, Shenyang 110016, PR China*

Received 3 July 2007; received in revised form 26 December 2007; accepted 16 January 2008
Available online 26 January 2008

Abstract—Syntheses of oligosaccharides expressed on cells are indispensable for the improvement of the functional analyses of the oligosaccharides and their applications. We are developing saccharide primers for synthesizing oligosaccharides using living cells. In this study, dodecyl 2-acetamido-2-deoxy-β-D-glucopyranoside (GlcNAc-C12) and dodecyl β-D-galactopyranosyl-(1→4)-2-acetamido-2-deoxy-β-D-glucopyranoside (LacNAc-C12) were examined for their abilities to prime the syntheses of neolacto-series oligosaccharides in HL60 cells. When GlcNAc-C12 was incubated with HL60 cells in serum-free medium for 2 days, 14 kinds of glycosylated products were collected from the culture medium. They were separated by high-performance liquid chromatography. The sequences of the products were determined to be neolacto-series oligosaccharides including Lewis^X, sialyl Lewis^X, polylactosamine, and sialylpolylactosamine by mass spectrometry. GlcNAc-C12 was also glycosylated by B16 cells and gave sialyllactosamine. Furthermore, LacNAc-C12 gave similar glycosylated products to GlcNAc-C12.

Keywords: Saccharide primer; *N*-Acetylglucosamine; *N*-Acetyllactosamine; Oligosaccharide; Glycosylation; Animal cells

1. Introduction

The importance of technology to synthesize oligosaccharides expressed on mammalian cells has been indicated by the elucidation of their roles in cell function. We have been developing saccharide primer methods to synthesize oligosaccharides using the glycan biosynthesis system in cells. A saccharide primer is a glycolipid analogue to be glycosylated by cells in culture. Yamagata and co-workers have developed amphiphilic glycolipid analogues such as alkyllactosides.[1,2] Dodecyl β-lactoside (Lac-C12) as a saccharide primer was incorporated into B16 melanoma cells and was glycosylated by glycosyltransferase. The glycosylated product was secreted from the cells. Structural analyses indicated that the product was sialyllactose, which is the carbohydrate portion of GM3 normally expressed on the surface of mouse B16 melanoma cells.

Other primers as substrates for glycosyltransferase in cells have been described in several reports. β-D-Xylosides have been developed as an initiator of glycosaminoglycan biosynthesis.[3,4] Acetylated Xylβ1-6Gal-*O*-2-naphthol and acetylated Galβ1-4GlcNAcβ-*O*-naphthalenemethanol (NM) were investigated as inhibitors of the glycosyltransferase in cells.[5] Furthermore, acetylated Galβ1-4GlcNAcβ-NM and acetylated GlcNAcβ1-3Galβ-NM inhibited the biosynthesis of endogenous sialyl Lewis^X, and they were also glycosylated in human promyelocytic leukemia HL60 cells.[6]

The glycosylation of the saccharide primers was suggested to be dependent on the cell lines, because different types of cells have different intrinsic glycan biosynthesis

*Corresponding author. Tel.: +81 45 566 1771; fax: +81 45 566 1447; e-mail: sato@bio.keio.ac.jp

0008-6215/$ - see front matter © 2008 Elsevier Ltd. All rights reserved.
doi:10.1016/j.carres.2008.01.022

systems. Therefore, a saccharide library could be synthesized by combining various saccharide primers and cells. HL60 cells are known to express ganglioside GM3 and neolacto-series oligosaccharides. When Lac-C12 was incubated with HL60 cells, only the sialylated product (sialyllactose) was obtained, but not neolacto-series oligosaccharides. Therefore, in the present study, we synthesized dodecyl 2-acetamido-2-deoxy-β-D-glucopyranoside (GlcNAc-C12) and dodecyl β-D-galactopyranosyl-(1→4)-2-acetamido-2-deoxy-β-D-glucopyranoside (LacNAc-C12) as saccharide primers (Fig. 1), and the glycosylation reactions of those primers by HL 60 cells and B16 cells were examined.

2. Results

2.1. Glycosylation of GlcNAc-C12 by HL60 cells

HL60 cells were employed to examine the usefulness of GlcNAc-C12 as saccharide primer for the synthesis of neolacto-series oligosaccharides. After incubation of 50 μM of GlcNAc-C12 with HL60 cells, glycosylated products and unreacted primers were collected from the culture medium and cell fraction using a Sep-Pak C_{18} column. The glycosylated products adsorbed to the column were eluted using mixed solvents of methanol and water. The glycosylated products were largely detected from the culture medium. The acidic and neutral products were eluted with 3:7 MeOH–H_2O, and 1:9 MeOH–H_2O, respectively. As shown in Figure 2A, HPTLC (high-performance thin-layer chromatography) indicated that the fractions eluted with 3:7 MeOH–H_2O contained four neutral products (N1–N4), and the fractions eluted with 1:9 MeOH–H_2O contained six acidic products (A1–A6). Next, the neutral and acidic products were separated by high-performance liquid chromatography (HPLC). The four neutral products were separated using 70:28:2 $CHCl_3$–MeOH–H_2O as shown in Figure 2B. N1, N2, N3, and N4 were detected in fraction numbers 7–9, 11–12, 35–40, and 70–80, respectively. The four acidic products (A1–A4) were separated using 70:28:2 $CHCl_3$–MeOH–H_2O as shown in Figure 2C. A1, A2, A3, and A4 were detected in fraction numbers 17–19, 20–23, 26–28, and 45–50, respectively. Two acidic products (A5–A6) were separated using 60:35:5 $CHCl_3$–MeOH–H_2O as shown in Figure 2D. A4 and A5 were detected in fraction numbers 10 and 11–13, respectively.

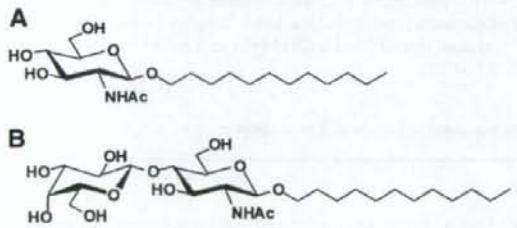

Figure 1. Saccharide primers, GlcNAc-C12 (A) and LacNAc-C12 (B), employed in this study.

2.2. Analyses of the chemical structures of products by mass spectrometry

Analyses of the structures of products separated by HPLC were carried out by MALDI-TOFMS (matrix-assisted laser desorption and ionization time-of-flight mass spectrometry). The observed masses and the deduced sequences of the glycosylated products are shown in Table 1. The mobility of N1 on HPTLC was same as that of synthetic Galβ1-4GlcNAc-C12 (LacNAc-C12), and the non-reducing hexose of N1 was cleaved by jack bean β-galactosidase (data not shown). Furthermore, the positive MALDI-PSD (post-source decay)

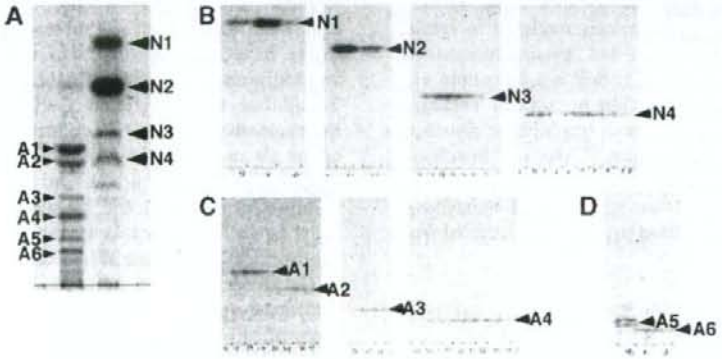

Figure 2. HPTLC of the products collected using a Sep-Pak C_{18} column (A), and purified by HPLC (B, C, and D) for the glycosylation of GlcNAc-C12 by HL60 cells.

Table 1. Deduced sequences and mass observed by MALDI-TOF-MS for the glycosylated products from GlcNAc-C12

Product	Sequence	Observed mass
N1	Galβ1-4GlcNAc-C12	574.1 $[M+Na]^+$
N2	Galβ1-4(Fucα1-3)-GlcNAc-C12	720.1 $[M+Na]^+$
N3	Galβ1-4GlcNAcβ1-3Galβ1-4GlcNAc-C12	939.1 $[M+Na]^+$
N4	Galβ1-4GlcNAcβ1-3Galβ1-4(Fucα1-3)GlcNAc-C12	1085.3 $[M+Na]^+$
A1	NeuNAcα2-3Galβ1-4GlcNAc-C12	841.4 $[M-H]^-$
A2	NeuNAcα2-6Galβ1-4GlcNAc-C12	841.4 $[M-H]^-$
A3	NeuNAc-(Galβ1-4GlcNAc)$_2$-C12	1230.1 $[M-H]^-$
A4	Fucose+A3	1376.3 $[M-H]^-$
A5	NeuNAc-(Galβ1-4GlcNAc)$_3$-C12	1595.9 $[M-H]^-$
A6	Fucose+A5	1742.0 $[M-H]^-$

spectrum (Table 2) revealed a peak at m/z 305.32 corresponding to $^{0,2}A_2$ fragment ($+Na^+$, intramolecular cleavage of GlcNAc). The results of MALDI-PSD agreed with the values in the literature.[7] Thus, N1 was determined to be Galβ1-4GlcNAc-C12. N2 was predicted to be H antigen (Fuc-Gal-GlcNAc-C12) or Lewis^X (Gal-(Fuc)-GlcNAc-C12) from the peak of m/z 720.1 ($[M+Na]^+$) of the MALDI-TOF-MS spectrum (Table 1). The MALDI-PSD spectrum of N2 (Table 2) revealed peaks at m/z 558.4 corresponding to $Y_{1\beta}$ (Fuc-GlcNAc-C12+Na^+) and m/z 305.4 corresponding to the $Y_{1\alpha}/^{0,2}A_2$ fragment ($+Na^+$). The observed fragment ions of N2 were similar to the MALDI-PSD spectrum of Lewis^X reported in the literature.[7] Therefore, N2 was determined to be Lewis^X. N3 was predicted to be Gal-GlcNAc-Gal-GlcNAc-C12 from the peak of m/z 939.1 ($[M+Na]^+$) of the MALDI-TOF-MS spectrum (Table 1). The MALDI-PSD spectrum of N3 (Table 2) revealed peaks at m/z 670.5 corresponding to $^{0,2}A_4$ fragment ($+Na^+$) and m/z 305.3 corresponding to $^{0,2}A_2$ fragment ($+Na^+$), suggesting the existence of two β-(1→4) lactosamine units. N4 was predicted to be fucosylated N3 from the peak of m/z 1085.3 ($[M+Na]^+$) of the MALDI-TOF-MS spectrum (Table 1). The MALDI-PSD spectrum of N4 (Table 2) revealed a peak at m/z 558.6 corresponding to $Y_{1\beta}$ (Fuc-GlcNAc-C12+Na^+), and fragmentation ions were similar to those of N3, suggesting that N4 is Galβ1-4GlcNAcβ1-3Galβ1-4(Fucα1-3)GlcNAc-C12. HL60 cells express FUT4, which transfers fucose to lactosamine.[8] Furthermore, it has been reported that FUT4 preferentially transfers fucose to inner GlcNAc residues.[9] The structure of N5 agreed with that of the endogenous glycan reported in the literature.[8,9]

Though the mobilities of A1 and A2 on HPTLC were different, the MALDI-TOF-MS spectra of them revealed the same mass of 841.4 ($[M-H]^-$), corresponding to NeuNAc-Gal-GlcNAc-C12 (sLacNAc-C12, Table 1). Since A1 and A2 are considered to have different linkages of *N*-acetylneuraminic acid to galactose, the

Table 2. Fragment ions observed by MALDI-PSD spectrum for the glycosylated products from GlcNAc-C12

Product	Fragments
N1	226.4 ($[Y_1/B_2+Na]^+$), 305.3 ($[^{0,2}A_2+Na]^+$), 388.4 ($[B_2+Na]^+$), 412.4 ($[Y_1+Na]^+$),
N2	226.3 ($[Y_{1\alpha}/Y_{1\beta}/B_2+Na]^+$), 305.4 ($[Y_{1\alpha}/^{0,2}A_2+Na]^+$), 370.5 ($[Z_1/B_2+Na]^+$), 388.3 ($[Y_{1\alpha}/B_2+Na]^+$), 412.4 ($[Y_{1\alpha}/Y_{1\beta}+Na]^+$), 534.4 ($[B_2+Na]^+$), 556.4 ($[Z_1+Na]^+$), 558.4 ($[Y_{1\beta}+Na]^+$), 574.6 ($[Y_{1\alpha}+Na]^+$)
N3	226.3 ($[Y_3/B_2+Na]^+$, $[B_4/Y_1+Na]^+$), 305.3 ($[^{0,2}A_2+Na]^+$), 388.2 ($[B_2+Na]^+$ or $[B_4/Y_2+Na]^+$), 406.4 ($[C_2+Na]^+$), 412.5 ($[Y_1+Na]^+$), 550.3 ($[B_3+Na]^+$), 574.5 ($[Y_2+Na]^+$), 670.5 ($[^{0,2}A_4+Na]^+$), 753.7 ($[B_4+Na]^+$), 777.9 ($[Y_3+Na]^+$)
N4	226.4 ($[Y_3/B_2+Na]^+$, $[Y_{1\alpha}/B_4/Y_{1\beta}+Na]^+$), 305.3 ($[^{0,2}A_2+Na]^+$), 388.5 ($[B_2+Na]^+$ or $[Y_{1\alpha}/B_4/Y_2+Na]^+$), 406.5 ($[C_2+Na]^+$), 412.7 ($[Y_{1\alpha}/Y_{1\beta}+Na]^+$), 550.6 ($[B_3+Na]^+$), 558.7 ($[Y_{1\beta}+Na]^+$), 574.9 ($[Y_{1\alpha}/Y_2+Na]^+$), 670.4 ($[Y_{1\alpha}/^{0,2}A_4+Na]^+$), 720.6 ($[Y_2+Na]^+$), 778.0 ($[Y_{1\alpha}/Y_3+Na]^+$), 901.9 ($[Y_3+Na]^+$), 940.0 ($[Y_{1\alpha}+Na]^+$)
A3	388.3 ($[Y_4/B_3+Na]^+$, $[Y_2/B_5+Na]^+$), 406.5 ($[Y_4/C_3+Na]^+$), 412.4 ($[Y_1+Na]^+$), 476.3 ($[B_2+Na]^+$), 550.5 ($[Y_4/B_4+Na]^+$), 574.6 ($[Y_2+Na]^+$), 634.9 ($[^{0,2}A_3+Na+K-H]^+$), 679.6 ($[B_3+Na]^+$), 753.8 ($[B_5/Y_3+Na]^+$), 777.7 ($[Y_3+Na]^+$), 939.8 ($[Y_4+Na]^+$)
A4	336.4 ($[B_1+2Na-H]^+$), 388.4 ($[Y_4/B_3+Na]^+$ or $[Y_{1\alpha}/Y_2/B_5+Na]^+$), 406.5 ($[Y_4/C_3+Na]^+$), 412.3 ($[Y_{1\alpha}/Y_{1\beta}+Na]^+$), 476.5 ($[B_2+Na]^+$), 550.6 ($[Y_4/B_4+Na]^+$), 558.9 ($[Y_{1\beta}+Na]^+$), 574.6 ($[Y_{1\alpha}/Y_2+Na]^+$), 634.9 ($[^{0,2}A_3+Na+K-H]^+$), 679.6 ($[B_3+Na]^+$), 720.9 ($[Y_2+Na]^+$), 777.8 ($[Y_{1\alpha}/Y_3+Na]^+$), 841.3 ($[B_4+Na]^+$), 923.9 ($[Y_3+Na]^+$), 939.6 ($[Y_{1\alpha}/Y_4+Na]^+$), 1085.4 ($[Y_4+Na]^+$), 1230.8 ($Y_{1\alpha}$)
A5	388.1 ($[Y_6/B_3+Na]^+$, $[B_5/Y_4+Na]^+$ or $[B_7/Y_2+Na]^+$), 406.2 ($[Y_6/C_3+Na]^+$ or $[C_5/Y_4+Na]^+$), 550.3 ($[B_6/Y_4+Na]^+$), 574.6 ($[Y_2+Na]^+$), 591.2 ($[Y_5/B_5+Na]^+$ or $[B_7/Y_4+Na]^+$), 596.7 ($[^{0,2}A_3+Na]^+$), 634.9 ($[^{0,2}A_3+Na+K-H]^+$), 670.2 ($[Y_6/^{0,2}A_5+Na]^+$, $[Y_4/^{0,2}A_7+Na]^+$), 679.5 ($[B_3+Na]^+$), 753.6 ($[Y_6/B_5+Na]^+$ or $[B_7/Y_4+Na]^+$), 777.6 ($[Y_3+Na]^+$), 916.8 ($[Y_4+H]^+$), 939.5 ($[Y_4+Na]^+$), 999.8 ($[^{0,2}A_5+Na]^+$), 1045.1 ($[B_5+Na]^+$), 1142.7 ($[Y_5+Na]^+$), 1305.0 ($[Y_6+Na]^+$)
A6	388.6 ($[Y_6/B_3+Na]^+$, $[B_5/Y_4+Na]^+$ or $[Y1_\alpha/B_7/Y_2+Na]^+$), 406.8 ($[Y_6/C_3+Na]^+$, $[C_5/Y_4+Na]^+$), 550.5 ($[B_6/Y_4+Na]^+$), 574.9 ($[Y_{1\alpha}/Y_2+Na]^+$), 591.3 ($[Y_5/B_5+Na]^+$ or $[Y_{1\alpha}/B_7/Y_3+Na]^+$), 596.2 ($[^{0,2}A_3+Na]^+$), 634.4 ($[^{0,2}A_3+Na+K+H]^+$), 720.2 ($[Y_2+Na]^+$), 753.8 ($[Y_{1\alpha}/Y_6/^{0,2}A_5+Na]^+$ or $[Y_{1\alpha}/Y_4/^{0,2}A_7+Na]^+$), 777.6 ($[Y_{1\alpha}/Y_3+Na]^+$), 899.9 ($[Y_4/B_7+Na]^+$), 916.9 ($[Y_{1\alpha}/Y_4+H]^+$), 923.9 ($[Y_3+Na]^+$), 939.8 ($[Y_{1\alpha}/Y_3+Na]^+$), 1000.0 ($[Y_{1\alpha}/^{0,2}A_5+Na]^+$), 1045.5 ($[B_5+Na]^+$), 1085.7 ($[Y_4+Na]^+$), 1288.8 ($[Y_5+Na]^+$), 1304.5 ($[Y_{1\alpha}/Y_6+Na]^+$), 1451.0 ($[Y_6+Na]^+$), 1472.6 ($[Y_6+2Na-H]^+$), 1596.1 ($[Y_{1\alpha}+Na]^+$)

enzymatic cleavages of sLacNAc-C12 by neuraminidases were examined. The neuraminidases employed in this study were *Arthrobacter ureafacience* neuraminidase, which hydrolyzes α-(2→3), α-(2→6), and α-(2→8) linkages,[10] and *Macrobdella decora* neuraminidase, which hydrolyzes α-(2→3) linkage.[11] Though *N*-acetylneuraminic acid of A1 was cleaved by both neuraminidases, that of A2 was cleaved by the *A. ureafacience* neuraminidase but not by the *M. decora* neuraminidase. The hydrolyzed products showed the same mobility as synthetic Galβ1-4GlcNAc-C12. Next, ESI (electrospray ionization)-CID (collision-induced dissociation) was employed to distinguish between A1 and A2. The ESI-CID spectra of A1 and A2 showed peaks of *m/z* 887.5 ($[M+2Na-H]^+$) corresponding to NeuNAc-Gal-GlcNAc-C12, and *m/z* 574.3 ($[(M\text{-anNeuNAc})+Na]^+$) corresponding to Y_2 fragment (Gal-GlcNAc-C12). The relative intensity of Y_2 (*m/z* 574.3) to the parent peak (*m/z* 887.5) showed significant differences between A1 and A2, and was 0.68 for A1 and 0.03 for A2. It has been reported that α-(2→3) sialyl linkage was distinguished from α-(2→6) sialyl linkage based on the ESI-CID spectra.[12] In the literature, the fragmentation ions produced by the cleavage of the α-(2→3) sialyl linkage showed much higher intensity than those produced by the cleavage of the α-(2→6) sialyl linkage. Therefore, from the results of enzymatic digestions and ESI-CID spectra, A1 and A2 were determined to be NeuNAcα2-3Galβ1-4GalNAc-C12 and NeuNAcα2-6Galβ1-4GalNAc-C12, respectively.

The MALDI-TOFMS spectra of A3 and A5 (Table 1) revealed peaks of *m/z* 1230.1 ($[M-H]^-$) corresponding to NeuNAc-(Gal-GlcNAc)$_2$-C12 and *m/z* 1571.7 ($[M-H]^-$) corresponding to NeuNAc-(Gal-GlcNAc)$_3$-C12. A3 was considered to be produced by the sialylation of N4. The MALDI-TOF-MS spectra of A4 and A6 revealed peaks of *m/z* 1352.7 ($[M-H]^-$) corresponding to fucosylated A3 and *m/z* 1779.0 ($[M-H]^-$) corresponding to fucosylated A5. The positive-ion mode MALDI-PSD spectrum of A4 (Table 2) revealed peaks at *m/z* 558.9 corresponding to $Y_{1\beta}$ (Fuc-GlcNAc-C12+Na^+) and *m/z* 720.9 corresponding to Y_2 (Fuc+Gal-GlcNAc-C12+Na^+). The positive-ion mode MALDI-PSD spectrum of A6 (Table 2) also revealed a peak at *m/z* 720.2 corresponding to Y_2 (Fuc+Gal-GlcNAc-C12+Na^+), *m/z* 923.9 corresponding to Y_3 (Fuc+GlcNAc-Gal-GlcNAc-C12+Na^+), and *m/z* 1085.7 corresponding to Y_4 (Fuc+Gal-GlcNAc-Gal-GlcNAc-C12+Na^+). These MALDI-PSD spectra suggested that the fucose moieties in A4 and A6 were linked to the innermost GlcNAc residue. It has been reported that HL60 cells express α-(1→3)-fucosyltransferase, and fucosylated monosialyl glycolipids having similar structures to A4 and A6 were detected in HL60 cells.[13] Though the linkages of *N*-acetylneuraminic acid in A3, A4, A5, and A6 could not be determined in the present study, they were inferred to be α-(2→3) from the structural analysis of the sialyl linkage of sialylpolylactosamine expressed in HL60 cells.[14]

2.3. Glycosylation of LacNAc-C12 by HL60 cells

Next, the glycosylation of LacNAc-C12 by HL60 cells was examined. After incubation of HL60 cells with 50 μM LacNAc-C12 for 2 days, glycosylated products and unreacted primer were isolated from the culture medium. The glycosylated products collected using a Sep-Pak C_{18} column were analyzed by HPTLC. One neutral product and six acidic products were detected. The analyses of mobility on HPTLC and the mass spectrum indicated that the products glycosylated from LacNAc-C12 were the same as those from GlcNAc-C12. The neutral product was N2 and the acidic products were A1–A6.

2.4. Comparison of GlcNAc-C12 and LacNAc-C12 as glycosyl acceptors in B16 cells

After incubation of 50 μM GlcNAc-C12 or LacNAc-C12 with B16 cells for 2 days, glycosylated products were isolated from the culture medium. The glycosylated products were analyzed by HPTLC and MALDT-TOF-MS. Using GlcNAc-C12, two glycosylated products were detected. One was Gal-GlcNAc-C12, whose mobility on HPTLC was the same as that of synthetic LacNAc-C12. The other was considered to be NeuNAc-Gal-GlcNAc-C12 (sLacNAc-C12) from the mass spectrum. For LacNAc-C12, the detected product was also suggested to be sLacNAc-C12 from the mobility on HPTLC and from the mass spectrum. To determine the linkage of the sialic acid, the product was treated with neuraminidases from *A. ureafaciens* and *M. decora*. Since the glycosylated product sLacNAc-C12 was hydrolyzed by both sialidases, the linkage of NeuNAc-Gal was determined to be α-(2→3). The amount of sLacNAc-C12 derived from GlcNAc-C12 was two times higher than that from LacNAc-C12, when the dose of saccharide primers was 50 μM (Fig. 3). The glycosylation efficiency of GlcNAc-C12 in cells was higher than that of LacNAc-C12 in cells. When the dose of GlcNAc-C12 was 50 μM (250 nmol), the amount of sLacNAc-C12 was determined to be 7.5 nmol by quantitative analysis using GM1 as standard.

2.5. Cell growth in the presence of saccharide primers

B16 cells were cultured in the absence and the presence of 50 μM GlcNAc-C12 and LacNAc-C12 for 2 days. The cell growth in the presence of the saccharide primers was almost similar to that of control (Fig. 4). Cell growth of HL60 cells was also investigated in the presence of 50 μM GlcNAc-C12 for 2 days (data not

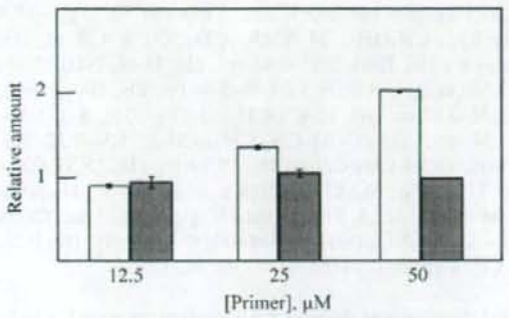

Figure 3. Relative amounts of NeuNAc-Gal-GlcNAc-C12 glycosylated from GlcNAc-C12 (white column) and Gal-GlcNAc-C12 (black column) by B16 melanoma cells (2×10^6 cells). The relative amounts were analyzed by densitometry at 540 nm followed by staining with resorcinol–HCl. The dose of saccharide primers was 50 μM.

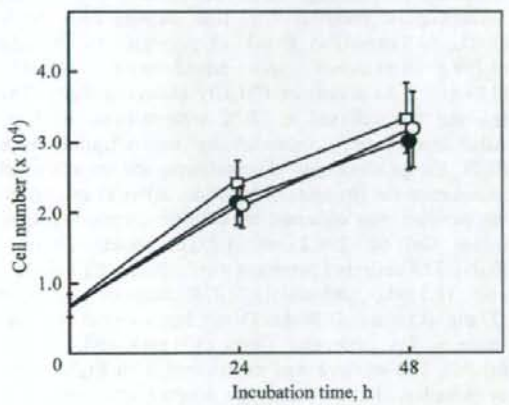

Figure 4. Growth of B16 cells cultured in the absence (closed circle) and the presence of 50 μM GlcNAc-C12 (open circle) and LacNAc-C12 (open square).

shown). The primers showed no cytotoxicity at the present experimental conditions.

3. Discussion

Convenient synthesis of glycan structures present on cells is important for the study to elucidate glycan function. Since saccharide primers can act as substrates for glycosyltransferases present in cells, they are useful for the synthesis of oligosaccharides expressed in cells. Saccharide primers are building blocks for constructing an oligosaccharide library by biocombinatorial synthesis that is combination of different saccharide primers and a variety of cells. It has been reported that Lac-C12, which is a mimicry of lactosylceramide, was useful to synthesize the oligosaccharides of glycosphingolipids (GSL). For example, Lac-C12 gave GM3 oligosaccharide when incubated with B16 melanoma cells. Furthermore, 12-azido dodecyl-β-lactoside (Lac-C12-N3) was synthesized with the aim of preparing glycan arrays or glycopolymers. Lac-C12-N3 was also glycosylated by cells as well as Lac-C12[15] and could be conjugated to solid supports by the modified Staudinger reaction or condensation reaction followed by reduction to the amino group for detecting carbohydrate recognition.[16]

For the construction of oligosaccharide libraries, it is important to synthesize various oligosaccharides. In our ongoing studies, it has been found that Lac-C12 gave rise to various oligosaccharides of ganglio- and globo-series gangliosides. Then, in the present study, we synthesized novel saccharide primers to selectively obtain neolacto-series oligosaccharides. In the biosynthesis of neolacto-series glycans, the lactosamine unit of Galβ1-4GlcNAc is the precursor region for sugar elongation. Thus, saccharide primers containing GlcNAc and LacNAc would be substrates for glycosyltransferases synthesizing neolacto-series oligosaccharides. In the literature, Esko and co-workers have reported that disaccharide primers such as peracetylated Galβ1-4GlcNAc-NM were fucosylated to Galβ1-4(Fucα1-3)GlcNAc-NM, and peracetylated GlcNAcβ1-3Gal-NM was converted to Galβ1-4(Fucα1-3)GlcNAcβ1-3Gal-NM, NeuNAcα2-3Galβ1-4GlcNAcβ1-3Gal-NM, and NeuNAcα2-3Galβ1-4(Fucα1-3)GlcNAcβ1-3Gal-NM by U937 human histiocytic lymphoma cells.[6] Those peracetylated primers were glycosylated after deacetylation in cells. In our study, deacetylated saccharide primer was used for the synthesis of oligosaccharides by cells. GlcNAc-C12 and LacNAc-C12 gave Le^X, sLe^X, polylactosamine, sialylated polylactosamine, and sialylated/fucosylated polylactosamine by incubating with HL60 cells. These oligosaccharides were similar to endogenous glycans observed in HL60.[17] The complex glycosylated products were clearly separated by HPLC, and their chemical structures were determined by enzymatic digestion and mass spectrometry. Separation and structural elucidation of the products were very convenient compared to the endogenous GSLs because the saccharide primers had a uniform aglycon structure.

Since GlcNAc-C12 gave similar glycosylated products to LacNAc-C12, we could conclude that monosaccharide primers as well as disaccharide primers are useful for the synthesis of oligosaccharides. It has been reported that the glycosylation efficiencies of saccharide primers were dependent on their hydrophilic–hydrophobic balance.[2,18] More hydrophilic saccharide primers cannot be internalized into cells, while more hydrophobic ones are strongly adsorbed to the cell membrane. Although the glycosylation efficiency of GlcNAc-C12 was higher than that of LacNAc-C12 in the present study, the structure for giving optimum glycosylation

efficiency would be determined by varying the hydrocarbon chain length.

In conclusion, saccharide primers such as GlcNAc-C12 and LacNAc-C12 were developed to synthesize neolacto-series oligosaccharides using mammalian cells. The glycosylated products were separated by HPLC, and the sequences were determined by enzymatic digestion and mass spectrometry. The saccharide primers employed in this study are expected to be useful for synthesizing oligosaccharides expressed in mammalian cells.

4. Experimental

4.1. Synthesis of dodecyl 2-acetamido-2-deoxy-β-D-glucopyranoside (GlcNAc-C12)

2-Acetamido-1,3,4,6-tetra-*O*-acetyl-2-deoxy-D-glucopyranoside (Ac_4-GlcNAc) was prepared by reacting *N*-acetylglucosamine (2.5 g, 11.3 nmol, GlcNAc, Sigma) with Ac_2O (15 mL, 159 mmol, Wako Pure Chemicals) in 30 mL of pyridine according to the literature.[19] Ac_4-GlcNAc (3 g, 7.71 mmol) was mixed with TMS-OTf (4.0 mL, 21.9 mmol, E. Merck) in CH_2Cl_2 under nitrogen.[20] The solution was refluxed at 50 °C with stirring for 7 h. After evaporation followed by neutralization with Et_3N, the product was chromatographed on silica gel to examine the progress of the reaction. The reaction mixture was mixed with 1-dodecanol (3.6 mL, 15.5 mmol, Wako Pure Chemicals), $BF_3{\cdot}OEt_2$ (21 mL, 7.9 mmol, Wako Pure Chemicals) in the presence of 4 Å molecular sieves (2.5 g), and stirred at room temperature for 22 h.[21] $BF_3{\cdot}OEt$ (20.1 mL, 0.79 mmol) was added at 18 h to complete the reaction. The mixture was neutralized with Et_3N. After evaporation, the product was purified by column chromatography (Silica Gel 60, E. Merck, 7 × 30 cm, 1:1 *n*-hexane–EtOAc). Yield: 63.8% (2.53 g). ^{1}H NMR($CDCl_3$): δ 5.51 (d, 1H, $J_{2,NH}$ 8.8 Hz, NH), 5.31 (dd, 1H, $J_{2,3}$ 10.1 Hz, $J_{3,4}$ 9.5 Hz, H-3), 5.06 (dd, 1H, $J_{3,4}$ 9.5 Hz, $J_{4,5}$ 9.9 Hz, H-4), 4.65 (d, 1H, $J_{1,2}$ 8.4 Hz, H-1), 4.26 (dd, 1H, $J_{5,6b}$ 4.7 Hz, $J_{6,gem}$ 12.3 Hz, H-6a), 4.12 (dd, 1H, $J_{5,6a}$ 2.4 Hz, $J_{6,gem}$ 12.3 Hz, H-6b), 3.89–3.75 (m, 2H, $J_{2,NH}$ 8.8 Hz, $J_{1,2}$ 8.4 Hz, H-2, $OCH_2CH_2(CH_2)_9CH_3$), 3.69 (ddd, $J_{4,5}$ 9.9 Hz, $J_{5,6a}$ 2,4 Hz, $J_{5,6b}$ 4.7 Hz, H-5), 3.50–3.42 (m, 1H, $OCH_2CH_2(CH_2)_9CH_3$), 1.94, 2.02, 2.02, and 2.08 (s, each 3H, Ac), 1.60–1.50 (m, 2H, OCH_2CH_2-$(CH_2)_9CH_3$), 1.35–1.14 (m, 18H, $OCH_2CH_2(CH_2)_9CH_3$), 0.87 (t, 3H,$OCH_2CH_2(CH_2)_9CH_3$).

Dodecyl 2-acetamido-3,4,6-tri-*O*-acetyl-2-deoxy-β-D-glucopyranoside (2.5 g, 4.85 mol) in 100 mL of MeOH was deacetylated in the presence of NaOMe (270 mg, 5.0 mmol, Wako Pure Chemicals). Deprotection was carried out with stirring for 40 min. After decolorization on charcoal in EtOH, the product GlcNAc-C12 was obtained by recrystallization in ethanol. Yield: 1.70 g (88.1%). Mp 160–162 °C, lit.[22] mp 161 °C, $[\alpha]_D$ −18.8 (*c* 0.12, CH_3OH). ^{1}H NMR (CD_3OD): δ 4.38 (d, 1H, $J_{1,2}$ 6.1 Hz, H-1), 3.91–3.83 (m, 2H, H-6a, NH), 3.70–3.58 (m, 2H, H-2, H-5), 3.48–3.40 (m, 2H, H-3, H-6b), 3.34–3.27 (m, 3H, H-4, OCH_2), 1.97 (s, 3H, Ac), 1.53–1.51 (m, 2H, $OCH_2CH_2(CH_2)_9CH_3$), 1.34–1.22 (m, 18H, $OCH_2CH_2(CH_2)_9CH_3$), 0.89 (t, 3H, OCH_2CH_2-$(CH_2)_9CH_3$). MALDI-TOFMS: calcd for $C_{20}H_{39}NO_6$: $(M+Na)^+$, 412.3, Found: $(M+Na)^+$, 412.3. Anal. Calcd for $C_{20}H_{39}NO_6{\cdot}0.3H_2O$ (398.68): C, 60.82; H, 10.11; N, 3.55. Found: C, 60.81; H, 10.04; N, 3.54.

4.2. Synthesis of dodecyl β-D-galactopyranosyl-(1→4)-2-acetamido-2-deoxy-β-D-glucopyranoside (LacNAc-C12)

2,3,4,6-Tetra-*O*-acetyl-β-D-galactopyranosyl-(1→4)-2-acetamido-1,3,6-tri-*O*-acetyl-2-deoxy-β-D-glucopyranoside (Ac-LacNAc) was prepared by mixing *N*-acetyllactosamine (982 mg, 2.56 nmol, LacNAc, Yaizu Suisankagaku Industry Co. Ltd, Japan) with Ac_2O (5 mL, 52.9 mmol) in 10 mL of pyridine. Ac-LacNAc (0.799 g, 1.88 mmol) was mixed with TMS-OTf (0.24 mL, 1.33 mmol) in CH_2Cl_2 under nitrogen. The solution was refluxed at 50 °C with stirring for 12 h. After evaporation, followed by neutralization with Et_3N, the product was chromatographed on silica gel to examine the progress of reaction. After evaporation, the product was collected by column chromatography (Silica Gel 60, 2 × 23 cm, 1:2:0.01 toluene–EtOAc–Et_3N). The collected products were mixed with 1-dodecanol (1.3 mL, 5.89 mmol), (*R*,*S*)-camphor sulfonate (27 mg, 0.12 mmol, Wako Pure Chemicals) in the presence of 4 Å molecular sieves (350 mg), and refluxed for 6 h. The mixture was neutralized with Et_3N. After evaporation of the solvent, the product was purified by column chromatography (Silica Gel 60, 2 × 35 cm, 2:3 *n*-hexane–EtOAc). Yield: 50% (478 mg). ^{1}H NMR ($CDCl_3$): δ: 5.63 (d, 1H, $J_{NH,2}$ 9.3 Hz, NH), 5.35 (d, 1H, $J_{3',4'}$ 2.9 Hz, H-4′), 5.11 (dd, 1H, H-2′), 5.06 (dd, 1H, $J_{3,4}$ 8.1 Hz, H-3), 4.97 (dd, 1H, $J_{2',3'}$ 10.3 Hz, H-3′), 4.51–4.46 (m, 2H, H-1′, H-6a), 4.43 (d, 1H, $J_{1,2}$ 7.3, H-1), 4.15–4.09 (m, 3H, H-6b, H-6b′, H-6a′), 4.03 (dd, 1H, $J_{2,3}$ 9.3 Hz, H-2), 3.87 (ddd, 1H, H-5′), 3.78 (dd, 1H, H-4), 3.62 (ddd, 1H, $J_{4,5}$ 5.6 Hz, H-5), 3.41 (dd, 2H, $OCH_2CH_2(CH_2)_9CH_3$), 2.15–1.96 (m, 21H, Ac), 1.60–1.46 (m, 2H, $OCH_2CH_2(CH_2)_9CH_3$), 1.30–1.18 (m, 18H, $OCH_2CH_2(CH_2)_9CH_3$), 0.87 (t, 3H, $OCH_2(CH_2)_{10}CH_3$).

Dodecyl 2,3,4,6-tetra-*O*-acetyl-β-D-galactopyranosyl-(1→4)-2-acetamido-3,6-di-*O*-acetyl-2-deoxy-β-D-glucopyranoside (478 g, 0.56 mmol) in 25 mL of MeOH was deacetylated by the addition of NaOMe (160 mg, 2.97 mmol) with stirring for 3 h. The reactant was concentrated after treating with Amberlite IR-120B (Organo Co., Japan). LacNAc-C12 was purified by distilling with EtOH, toluene, and $CHCl_3$. Yield: 326 mg